Reviews in Mineralogy & Geochemistry
Vol. 88 pp. 533–566, 2022

Pressure and Temperature Data for Diamonds

Paolo Nimis

Dipartimento di Geoscienze
Università di Padova
via G. Gradenigo 6, 35131 Padova, Italy

paolo.nimis@unipd.it

INTRODUCTION

One of the key scientific questions about diamonds is "how are they formed?" To answer this question, we need to know the diamond-forming reactions and the physicochemical conditions under which these reactions take place. The pressure (*P*) and temperature (*T*) of diamond formation are an essential part of this knowledge and their assessment is pivotal to develop predictive scenarios of diamond distribution in the Earth interior. These scenarios may contribute to our understanding of global Earth processes, such as the long-term carbon cycle, and might also eventually improve our capability to select potential targets for diamond exploration (Shirey et al. 2013; Nimis et al. 2020).

The evaluation of the *P* and *T* of diamond formation can be carried out at two levels of investigation. The first is concerned with formation conditions for individual diamonds or small populations of diamonds from specific sources. This approach has been so far the most widely practiced. The second level considers the statistical distribution of *P–T* conditions for diamond formation at either local or global scale. This type of investigation is hampered by the difficulty of obtaining large sets of suitable samples from a specific locality or for a statistically significant number of localities, and is therefore unavoidably affected to some degree by sampling bias. Despite inherent limitations, the latter approach is the most appropriate to reveal systematics in diamond *P–T* distributions and, ultimately, in diamond depth distribution within the Earth.

Early reviews of *P–T* distributions for lithospheric diamonds were made by Nimis (2002), based on thermobarometry of chromian diopside inclusions, and by Stachel and Harris (2008) and Stachel (2014), using a more comprehensive set of thermobarometers. More recently, Nimis et al. (2020) investigated diamond depth distributions for a set of South African kimberlites and provided evidence for systematic trends of likely global significance. The depth distribution for sublithospheric diamonds worldwide was reviewed by Harte (2010). In this contribution, I first describe the methods that can be used to estimate the *P–T* conditions of diamond formation, highlighting their respective strengths and weaknesses. I then review existing diamond *P–T* data and their implications for diamond distribution with depth from both a local and a global perspective.

METHODS FOR DIAMOND THERMOBAROMETRY

Thermobarometry of diamonds can be carried out by estimating *P–T* conditions of chemical or elastic equilibrium of mineral inclusions contained within them. With some assumptions, the aggregation state of nitrogen substituting for carbon in the diamond lattice can also be used as a thermometer. In some cases, it is possible to derive both *P* and *T* estimates for a diamond by combining independent thermobarometric methods. In most instances, however, either *P*

1529-6466/22/0088-0010$05.00 (print)
1943-2666/22/0088-0010$05.00 (online)
http://dx.doi.org/10.2138/rmg.2022.88.10

or *T* estimates can be directly retrieved with sufficient confidence. Below is a list of currently available methods for diamond thermobarometry. Those based on chemical equilibria are specific for different minerals or mineral pairs. Since many inclusions in diamonds occur as isolated grains, detached from their original mineral assemblage, particular emphasis is given in this review to methods that use single minerals to retrieve *P* and/or *T*. The following descriptions emphasize thermobarometry applications rather than principles, and the reader is referred to the original publications for details of the specific thermobarometers.

Thermometry

Pyroxenes. Many ultramafic mantle rocks contain both clinopyroxene and orthopyroxene. This mineral pair forms one of the most widely used geological thermometers, which is based on the net-transfer reaction of the enstatite component between the two pyroxenes $MgSiO_3$(Opx) ↔ $MgSiO_3$(Cpx). The very small *P*-dependency of this reaction limits propagation of errors when *T* is calculated by iteration in combination with an independent barometer. Several versions of this thermometer have been proposed in the literature. Tests based on experimental results and pyroxene compositions in natural xenoliths suggest that the calibration of Taylor (1998) is the most reliable for mantle peridotites and pyroxenites in a *T* range of 700 to at least 1400 °C (Nimis and Grütter 2010), which covers the entire range of the lithospheric diamond window. The much more popular Brey and Köhler (1990) calibration gives similar results for clinopyroxenes with relatively low Na contents around 0.05 atoms per 6-oxygen formula unit (apfu), but was proven to overestimate with increasing Na_{Cpx} (e.g., +150 °C at Na_{Cpx} = 0.25 apfu; Nimis and Grütter 2010). For inclusions in diamonds and diamond-bearing peridotitic xenoliths (average Na_{Cpx} = 0.12 apfu, median = 0.09 apfu, standard deviation = 0.08 apfu), the Brey and Köhler (1990) calibration will yield estimates that are on average ~50 °C higher that those using the Taylor (1998) calibration. Larger discrepancies may be expected for unusually Na-rich clinopyroxenes.

Since clinopyroxene–orthopyroxene inclusion pairs are very rare in diamonds, it is generally more practical to use the alternative single-clinopyroxene version of Nimis and Taylor (2000). The two-pyroxene Taylor (1998) and single-clinopyroxene Nimis and Taylor (2000) methods provide almost indistinguishable results when applied to mantle ultramafic rocks that contain both pyroxenes (Nimis and Grütter 2010). Although the Nimis and Taylor (2000) thermometer uses only one pyroxene to calculate *T*, its application expressly requires that both pyroxenes were part of the mineral assemblage and were in chemical equilibrium. Therefore, this method is only suitable for diamonds belonging to the lherzolitic or websteritic suites and containing clinopyroxene inclusions, either isolated or associated with other minerals. If orthopyroxene was not part of the original mineral assemblage, as is the case for wehrlitic inclusions, single-clinopyroxene thermometry would only provide a minimum *T* estimate. An anomalously low *T* estimate (e.g., one that lies much below the local geotherm) may be a sign that the clinopyroxene is wehrlitic. Ziberna et al. (2016) suggested that a Ca/(Ca + Mg) molar ratio of > 0.5 should also be considered as suspicious, as only ~1% of orthopyroxene-saturated mantle clinopyroxenes lie above this value. Nonetheless, discrimination of wehrlitic clinopyroxenes is not generally possible based merely on compositional criteria.

Simakov (2008) proposed a different, more complex calibration of the single-clinopyroxene thermometer, which definitely improves performance above 1500 °C, though not over the *T* < 1400 °C range typical of 'lithospheric' temperatures (note that the $T_{\text{Nimis and Taylor 2000}}$ estimates reported in Fig. 10 of Simakov 2008 are incorrect and unduly suggest overestimation below 1300 °C).

The Ca-in-Opx thermometer of Brey and Köhler (1990) is the single-orthopyroxene version of the pyroxene thermometer and can provide estimates that are complementary to, and independent from those obtained with the single-clinopyroxene thermometer. The two single-pyroxene methods were shown to be mutually consistent, provided a correction is applied

below 900 °C (Nimis and Grütter 2010). However, since inclusions of likely harzburgitic (i.e., clinopyroxene-free) affinity are relatively common in diamonds (Stachel and Harris 2008), the possibility that $T_{Ca\text{-}in\text{-}Opx}$ estimates for orthopyroxene inclusions are only minimum *T* values is much higher than for the single-clinopyroxene thermometer. Therefore, its usefulness is rather limited in diamond studies.

Garnet. The Ni content of garnet in equilibrium with olivine is very sensitive to *T* and apparently independent of *P* (Ryan et al. 1996; Canil 1999). Since the Ni content of olivine shows small variations in both mantle xenoliths (O'Reilly et al. 1997) and inclusions in diamonds (Griffin et al. 1992; Sobolev et al. 2008), *T* can be retrieved from Ni_{garnet} alone, by assuming an appropriate Ni content for coexisting forsteritic olivine. A useful reference values for $Ni_{olivine}$ is the mean value for mantle olivines (mean ± standard deviation = 2900 ± 360 ppm; Ryan et al. 1996), which is also close to the average value for olivine inclusions in diamonds worldwide (Stachel and Harris 2008; Sobolev et al. 2009). If available, the mean $Ni_{olivine}$ value for olivine inclusions in diamonds from the same locality may be used (e.g., 3150 ± 200 ppm for 51 inclusions from the Kalahari craton, Griffin et al. 1992; 2700 ppm for 88 inclusions from Arkhangel'sk province, Malkovets et al. 2011). Choosing one or the other value changes the final *T* estimate by at most a few tens of degrees (Fig. 1). The concentrations of Ni_{garnet} can be measured with a laser-ablation inductively-coupled plasma mass spectrometer (LA-ICP-MS), an ion microprobe (SIMS) or a proton microprobe (PIXE), which typically ensure a precision within a few ppm. The assumption of equilibrium with olivine may require compositional filtering (e.g., Grütter et al. 2004) to exclude any non-peridotitic garnet.

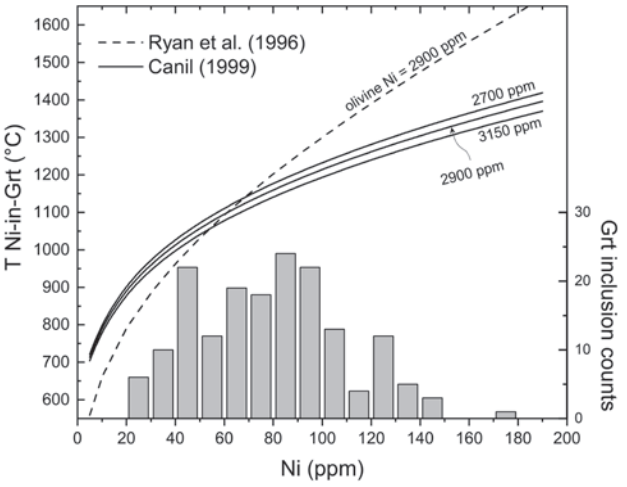

Figure 1. Relationships between Ni contents in garnet and calculated temperatures using the Ni-in-Grt thermometers of Ryan et al. (1996) and Canil (1999). The Ryan et al. (1996) version assumes a Ni content in olivine of 2900 ppm. Temperatures for the Canil (1999) version were calculated assuming a Ni content in coexisting olivine equal to the average for mantle olivines (2900 ppm) and to the average for olivine inclusions in Kalahari diamonds (3150 ppm) and in Arkhangel'sk diamonds (2700 ppm), respectively. The frequency distribution for 171 Cr-pyrope inclusions in diamonds from various localities (Griffin et al. 1992, 1993; Davies et al. 2004a; Viljoen et al. 2014; De Hoog et al. 2019) is shown for comparison, excluding two outliers at 236 and 431 ppm Ni.

The Ni-in-garnet thermometer has seen wide application in studies of Cr-pyrope garnets included in diamonds (e.g., Griffin et al. 1992, 1993; Davies et al. 2004a; Viljoen et al. 2014; De Hoog et al. 2019). Its calibration, however, is somewhat controversial. Ryan et al. (1996)

calibrated it against mantle xenoliths, using *T* values derived from a combination of the olivine–garnet Fe–Mg-exchange thermometer (O'Neill and Wood 1979) and the MacGregor (1974) and Brey and Köhler (1990) orthopyroxene–garnet barometers. Canil (1999) calibrated it against experiments at $T \geq 1200$ °C. The two calibrations give identical results at ~1100 °C, but progressively diverge at lower and higher *T* (Fig. 1). As a result, estimates obtained through the Canil (1999) formulation will typically span over narrower *T* intervals. Considering the most typical range for Ni in garnet inclusions, the maximum difference T_{Canil}–T_{Ryan} is ca. +100 °C at 20 ppm Ni and ca. –250 °C at 180 ppm Ni. It has been variously claimed that either calibration, or even their 'average', agree best with other independent thermometers when applied to mantle xenoliths (e.g., Ryan et al. 1996; Canil 1999; De Hoog et al. 2019; Czas et al. 2020; Nimis et al. 2020), but a definitive assessment using internally consistent thermobarometers as reference is still lacking. The latest attempt to refine the Ni-in-garnet thermometer was made by Sudholz et al. (2021a), who recalibrated it against new experiments in a relatively narrow *T* range (1100–1325 °C) and introduced correction terms for Ca and Cr contents in the garnet. When tested against independent estimates for xenoliths using the Nimis and Taylor (2000) enstatite-in-clinopyroxene thermometer, the Sudholz et al. (2021a) calibration shows improved overall accuracy above 1100 °C relative to the Canil (1999) experimental calibration, but poorer overall precision and slightly stronger progressive overestimation at lower *T* (see Fig. 7 in Sudholz et al. 2021a).

The Mn content of garnet in equilibrium with mantle olivine is sensitive to *T* (Smith et al. 1991) and can be used as a single-mineral thermometer, assuming a constant Mn content in olivine. This thermometer relies on electron microprobe data and was proposed as a substitute for the Ni-in-garnet thermometer when trace element data are not available (Grütter et al. 1999; Creighton 2009). The declared precision is rather poor (mostly ±150 °C) and, in the absence of independent olivine data, severe underestimation may occur at high *T*. Therefore, this method may have some use in surveys of large populations of garnet xenocrysts recovered during diamond exploration (e.g., Grütter and Tuer 2009), but its utility for diamond thermobarometry is limited.

Ashchepkov et al. (2010) calibrated two monomineral thermometers for garnets in equilibrium with clinopyroxene or olivine, respectively. These methods are simplified versions of Fe–Mg-exchange thermometers for clinopyroxene–garnet or olivine-garnet pairs, in which the clinopyroxene and olivine compositions are modeled from the composition of the garnet. Their accuracy cannot be better than that of the original two-mineral formulations, which are problematic themselves (see below). Also, *P* must be independently known to calculate *T*. In a test on mantle xenoliths from the Udachnaya kimberlite, these thermometers reproduced temperatures calculated with the pyroxene thermometer of Brey and Köhler (1990), at pressures calculated with the orthopyroxene–garnet barometer, to within ca. ±100 °C. Additional uncertainties due to problematic estimation of *P* in the absence of compositional data for coexisting orthopyroxene (see below) probably make these thermometers of little interest for diamond thermobarometry, especially when investigating small populations of diamonds.

Olivine. The Al content in peridotitic olivine is sensitive to *T* and can be used as a thermometer. The first Al-in-olivine thermometer for peridotitic olivine at conditions relevant to diamond was empirically calibrated on mantle xenoliths by De Hoog et al. (2010), using *P–T* estimates derived by a combination of the two-pyroxene thermometer and orthopyroxene–garnet barometer of Brey and Köhler (1990). The method was recalibrated by Bussweiler et al. (2017) by analysis of olivine from high-*P–T* experimental charges. The Al content in cratonic mantle olivine ranges from ~1 ppm to ~250 ppm and is conveniently analyzed by techniques such as LA-ICP-MS or SIMS, which ensure a precision within a few ppm. Electron microprobe analysis (EMPA) using very high probe currents (e.g., ≥ 200 nA) and long count times (≥ 100 s) may be a valid alternative (Batanova et al. 2018; D'Souza et al. 2020).

Al-in-olivine temperatures for spinel peridotites or strongly metasomatized garnet peridotites may be significantly underestimated or, respectively, overestimated. Compositional screening using an Al vs V diagram may help to discriminate these 'unsafe' olivines (Bussweiler et al. 2017). Screening is especially important if olivine is not physically associated with garnet, as occurs with many inclusions in diamonds. The Al-in-olivine thermometer gives systematically higher estimates (~50 °C, slightly increasing below 900 °C) than the single-clinopyroxene thermometer (Nimis and Taylor 2000) for natural mantle peridotites, probably reflecting slight suppression of Al incorporation in the experimental olivines due to Na loss (Bussweiler et al. 2017). The discrepancy is sufficiently small to ensure successful application of the method, but should be considered when comparing estimates obtained using different thermometers. The Al-in-olivine thermometer has not yet been widely used in diamond studies (see Korolev et al. 2018 for an example of application), owing to its recent development and the necessity of non-routine analysis of Al. Considering the great abundance of olivine among inclusions in diamonds (Stachel and Harris 2008), its application is likely to increase significantly in the future.

Spinel. The Zn content of spinel in equilibrium with mantle olivine is sensitive to *T*. Since the Zn content of mantle olivine is nearly constant (mean ± standard deviation = 52 ± 14 ppm), the Zn content of spinel can directly be used as a thermometer (Ryan et al. 1996). The concentrations of Zn in spinel can be measured by SIMS or PIXE, which ensure a precision within a few ppm. The current version of the Zn-in-spinel thermometer was calibrated over the range 680–1180 °C against *T* for coexisting garnets using the Ryan et al. (1996) version of the Ni-in-garnet thermometer. Therefore, it is subject to at least the same uncertainties as the Ni-in-garnet thermometer (see above).

Fe–Mg exchange thermometers. These popular thermometers are based on the distribution of Fe^{2+} and Mg between two mineral phases and can be used to derive *T* for inclusions in which garnet is associated with olivine, orthopyroxene or clinopyroxene. Tests using mineral compositions from mantle xenoliths and experiments showed that these thermometers suffer from either low precision or systematic errors or both (see review of Nimis and Grütter 2010). In peridotitic systems, the olivine-garnet and the clinopyroxene–garnet thermometers show the lowest precision, with possible discrepancies exceeding 200 °C. The Harley (1984) orthopyroxene–garnet formulation shows the highest precision, but systematically overestimates at $T < 1100$ °C and underestimates at $T > 1100$ °C (by up to ~150 °C, on average, for mantle xenoliths). All these discrepancies may reflect a modest sensitivity to *T* of the exchange reaction (particularly for olivine-garnet), oversimplification in the solid solution models used (especially for garnet and clinopyroxene), and $Fe^{3+}/\Sigma Fe$ ratios in the minerals different from those in the calibration samples. Matjuschkin et al. (2014) experimentally demonstrated the large effect of neglected Fe^{3+} on orthopyroxene–garnet and olivine-garnet thermometers. Their experiments in the Na-free $CaO–FeO–Fe_2O_3–MgO–Al_2O_3–SiO_2$ system at 5 GPa and 1000–1400 °C suggest that temperature estimates may be significantly improved if calculations are made using Fe^{2+} instead of total Fe in the garnet. Mössbauer data for orthopyroxene and garnet in peridotitic xenoliths, however, suggest that the partitioning of Fe^{3+} between these two minerals is affected by pressure and Na content in the orthopyroxene (Nimis et al. 2015). Therefore, a test over a range of relevant pressures in a Na-bearing system would be desirable. Nimis and Grütter (2010) empirically corrected the Harley (1984) thermometer using two-pyroxene thermometry of well equilibrated mantle xenoliths as calibration. The corrected version generally yields lower *T* estimates at low *T* and higher *T* estimates at high *T* relative to the uncorrected thermometer and may be more accurate for orthopyroxene–garnet pairs equilibrated under 'average' mantle redox conditions. On the other hand, it may produce large errors (> to $\gg$100 °C) if redox conditions are far from 'average', especially for strongly oxidized conditions at very high pressure and when both *P* and *T* are calculated by iteration in combination with an orthopyroxene–garnet barometer (Nimis et al. 2015). Considering that

at deep lithospheric levels diamond is stable over a relatively wide range of redox conditions ($\Delta\log fO_2$ FMQ ≈ –5 to –2), this problem can be serious. Also, application to some xenolith suites tends to produce frequent high-*P*–*T* outliers (Grütter, pers. comm.). In spite of its recognized systematic discrepancies, the original Harley (1984) version may still be preferable for diamond thermobarometry due to its lower *P* dependence, which reduces error propagation during iterative *P*–*T* calculations. However, the systematic deviations of the Harley (1984) thermometer at *T* far from 1100 °C, especially if all Fe is treated as Fe^{2+}, should be considered in data evaluation.

The clinopyroxene–garnet thermometer represents the only viable method to determine *T* from major element compositions of eclogitic inclusions in diamonds. There are many versions of this thermometer in the literature. The most recent calibration (Nakamura 2009) is based on an expanded experimental database covering mafic and ultramafic compositions across the *P* and *T* ranges relevant to diamond (1.5–7.5 GPa, 800–1820 °C) and incorporates updated solid solution models for both clinopyroxene and garnet. Older, more simplified, but in some cases still very popular versions of this thermometer do not reproduce the same experiments equally well and often show systematic deviations with changing *T* and composition. The nominal uncertainty of the Nakamura (2009) thermometer (±74 °C at the 1-sigma level) is still about double that of the best performing thermometers for peridotitic inclusions. None of the available versions of the clinopyroxene–garnet thermometer include corrections for the content of jadeite in clinopyroxene, therefore application to clinopyroxenes with Na > 0.5 apfu is not recommended. This excludes 15% of reported compositions for inclusions in eclogitic diamonds. As regards the Fe^{3+} problem, Purwin et al. (2013) and Matjushkin et al. (2014) measured $Fe^{3+}/\Sigma Fe$ ratios of coexisting clinopyroxenes and garnets in a CaO–FeO–Fe_2O_3–MgO–Al_2O_3–SiO_2 system at 2.5–5.0 GPa and 800–1400 °C and found no systematic deviations in the results of clinopyroxene–garnet Fe–Mg-exchange thermometry using the Krogh (1988) thermometer when all Fe was treated as Fe^{2+}. However, since the system investigated was Na-free, it did not allow for the incorporation of Fe^{3+} in clinopyroxene as aegirine component. This mechanism was shown to be relevant in clinopyroxenes from garnet peridotites (Woodland 2009) and may be even more so in eclogitic clinopyroxenes. The effect of Na on Fe^{3+} uptake in clinopyroxene probably contributes to the lower precision of the clinopyroxene–garnet thermometer in applications to natural samples.

Trace element-based clinopyroxene–garnet thermometers. The partitioning of REE between clinopyroxene and garnet is sensitive to *T* and has been used as a base for a clinopyroxene–garnet thermometer (Witt-Eickschen and O'Neill 2005; Sun and Liang 2015; Pickles et al. 2016). A possible advantage of REE thermometry over classical Fe–Mg-exchange thermometry is that REE diffusivity is small compared to that of Fe and Mg. Therefore, REE thermometry is predictably more robust against reequilibration of touching inclusions in diamonds during kimberlite transport or subsequent cooling. The version by Pickles et al. (2016) is particularly interesting, as it is independent of other thermometers and reproduces experimental temperatures moderately well (mean deviation of ±76 °C) with a small *P* dependence (~50 °C/1 GPa). This method is also independent of variations in $Fe^{3+}/\Sigma Fe$ ratio and may thus pose a promising alternative to the traditional clinopyroxene–garnet Fe–Mg exchange thermometer. A practical disadvantage is the requirement of high-quality REE data, which cannot be obtained with routine electron microprobe analysis. To the author's knowledge, there are no *T* data for diamonds using this method.

Nitrogen-aggregation thermochronometry. Nitrogen is the most common impurity in natural diamonds. With time, nitrogen atoms in the diamond crystal lattice tend to aggregate, proceeding from initial C-centers (single nitrogen) in Type Ib diamond, to A-centers (nitrogen pairs) in Type IaA diamond and, finally, to B-centers (nitrogen in tetrahedral arrangement) in Type IaB diamond. The first transformation is completed in relatively short geological times (for a N

content of 1000 ppm: ~100 yr at 1350 °C, and ~16 m.y at 950 °C; Taylor et al. 1996). Therefore, most natural diamonds are of the intermediate IaAB variety, the proportion of B-centers being a function of nitrogen content, temperature and time (Taylor et al. 1990; Mendelssohn and Milledge 1995). If the ages of the diamond and of its host kimberlite are known, one can calculate the integrated average temperature under which the diamond has resided in the mantle since its formation, i.e., the mantle residence temperature, T_{res}. Radiometric dating of inclusions within a particular diamond is rarely available. More commonly, the age of the diamond is assumed on the basis of radiometric dating of other diamonds from the same source. However, nitrogen aggregation is much more sensitive to temperature than to time and can be used as an effective thermometer, assuming the diamond has resided in the mantle at constant T since formation (Taylor et al. 1990, 1996). A diagram of nitrogen content vs the relative percentage of B-centers permits appreciation of age uncertainties on thermometry, since isotherms can be drawn for different mantle residence times (Fig. 2). Chronometry errors of one b.y. propagate thermometry errors of only a few tens of degrees on calculated T_{res}, unless the diamond is unusually young.

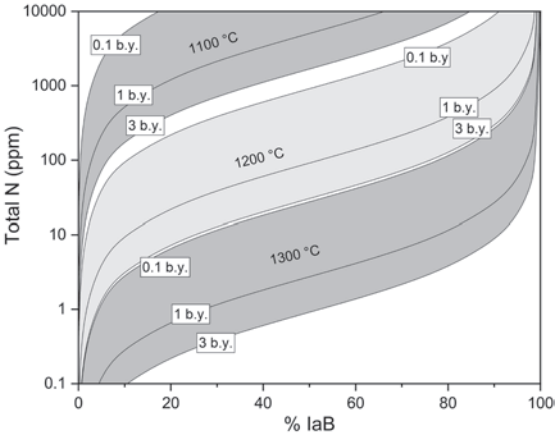

Figure 2. Plot of total nitrogen content in diamond vs percentage of nitrogen as B-centers. Mantle residence isotherms (1100, 1200 and 1300 °C) are calculated for residence times of 0.1, 1 and 3 b.y. (Taylor et al. 1990), using E_a = 7.0 eV and ln(A) = 12.59 (Taylor et al. 1996).

Nitrogen content and aggregation can be measured by Fourier-Transform Infrared (FTIR) spectroscopy, using an infrared microscope in transmission mode. This method logically provides nitrogen content and aggregation data averaged over the volume of diamond analyzed. Working on thinned (ideally, a few hundred μm) samples at high spatial resolution may help to detect zoning and to obtain more robust estimates from distinct diamond growth zones. The reader is referred to Kohn et al. (2016) for practical guidelines on spatially resolved FTIR thermochronometry and for interpretation of data for zoned diamonds. Detection limits for nitrogen content in diamonds are typically on the order of 5–10 ppm for high-quality spectra. Nitrogen contents below detection limit (Type-II diamonds) are relatively rare in lithospheric diamonds, but are more common in sublithospheric diamonds and are clearly unsuitable for nitrogen-aggregation thermochronometry. It must be clear that, contrary to thermodynamic equilibria used in inclusion thermobarometry, nitrogen aggregation is a kinetic process and so does not provide a snapshot of temperature conditions at a certain time. For instance, a short period of elevated temperature, e.g., due to circulation of hot fluids in the mantle during or after diamond growth, may have a large effect on nitrogen aggregation and could lead to ambiguous interpretations of calculated T_{res}. In general, unless the diamond is very young relative to its kimberlite host, heating on a time

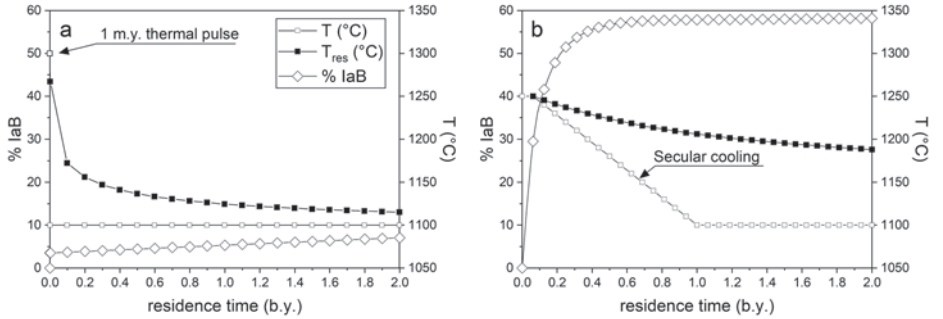

Figure 3. Variation of nitrogen aggregation and calculated T_{res} vs. mantle residence time for two diamonds with different thermal histories. (**a**) Diamond is formed at 1300 °C during a short-term (1 m.y) thermal pulse, followed by rapid return to ambient conditions of 1100 °C. Unless the residence time is very short, T_{res} rapidly diverges from the formation T. After a few 100 m.y., T_{res} approaches final ambient conditions. Note that the timing of the short thermal pulse does not influence the values of T_{res} that are calculated after the pulse at any given residence time. (**b**) Diamond formation at 1250 °C is followed by secular cooling to 1100 °C over a 1 b.y. period and then by constant T conditions for a further 1 b.y. The apparent T_{res} remains close to the formation T for short residence times, but progressive underestimation of formation T occurs with increasing time.

scale of ~1 m.y. will have small effects on the calculated T_{res}, which will approach ambient mantle conditions rather than conditions during diamond formation (Fig. 3a). If the diamond experienced secular cooling over a b.y. time scale subsequent to formation, the calculated T_{res} may both significantly underestimate the formation T and overestimate the final ambient T (Fig. 3b).

Barometry

Orthopyroxene–garnet. The Al content of orthopyroxene in equilibrium with garnet is strongly sensitive to P and forms the basis of the most widely used barometer for garnet-bearing peridotites. In this barometer, P mostly depends on the Al content in the orthopyroxene, but the compositions of both minerals must be considered to obtain robust estimates. Of the many calibrations of this barometer, that of Brey and Köhler (1990) is by far the most popular, but the older Nickel and Green (1985) calibration reproduces experimental pressures for most peridotitic systems to somewhat better precision (Nimis and Grütter 2010). Still, the Nickel and Green (1985) version was formulated under simple model-system assumptions and requires correction of Al-component activity to avoid P underestimation for orthopyroxenes with non-negligible contents of jadeite component. Carswell and Gibb (1987) and Carswell (1991) proposed two simple correction schemes, based on different assumptions on how Ti is coupled with Na and Al in orthopyroxene. The two corrections only apply to orthopyroxenes with $Na > (Cr + Fe^{3+} + 2{\cdot}Ti)$ or, respectively, $Na > (Cr + Fe^{3+} + Ti)$ atoms per formula unit, Fe^{3+} usually being neglected in practical applications. That of Carswell and Gibb (1987), which was also adopted by Brey and Köhler (1990) for their barometer, produces slightly smaller P variations, but there is as yet no solid experimental basis to prefer one correction over the other. The T-dependence of the orthopyroxene–garnet barometer is reasonably small (~0.2–0.3 GPa / 50 °C), but still sufficiently large to require an accurate independent estimate of T. This fact should be considered when this barometer is used in combination with the Harley (1984) orthopyroxene–garnet thermometer, which is known to overestimate at low T and underestimate at high T (see above): the artificial compression of T estimates produced by the Harley (1984) thermometer will necessarily result in non-natural compression also of P estimates. In general, errors in input T will displace the calculated P–T estimates roughly along a typical cratonic geotherm, thus limiting the 'apparent' scatter in P–T plots for samples equilibrated on the geotherm (Fig. 4). This may be an advantage if the aim is to define the mantle geotherm, but may give the misperception of a high overall precision by masking the true dispersion of the data.

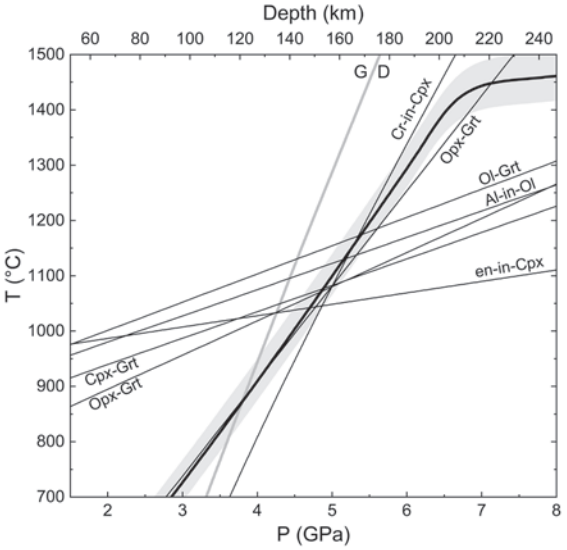

Figure 4. *P* and *T* dependence for some of the most widely used thermometers and barometers suitable for inclusions in diamonds, using typical inclusion compositions. Thermometers: Cpx–Grt – Nakamura (2009); Opx–Grt – Harley (1984), en-in-Cpx– Nimis and Taylor (2000); Al-in-Ol – Bussweiler et al. (2017); Ol–Grt – Wu and Zhao (2007). Barometers: Opx–Grt – Nickel and Green (1985); Cr-in-Cpx – Nimis and Taylor (2000). The thick solid line with 95% confidence bands is an example of a typical model cratonic geotherm calculated with FITPLOT from xenolith *P–T* data (Mather et al. 2011). GD: the graphite–diamond boundary after Day (2012).

Clinopyroxene–garnet. Barometry of bimineralic eclogites and of eclogitic clinopyroxene–garnet inclusion pairs in diamonds has long been a problem for mantle scientists. There have been several attempts to develop a suitable barometer based on the *P*-sensitive equilibrium grossular + pyrope ↔ diopside + Ca-Tschermak. According to a recent test by Beyer et al. (2018), the Beyer et al. (2015) formulation reproduces pressures for experiments in natural systems significantly better than the earlier formulations of Simakov and Taylor (2000) and Simakov (2008). Nonetheless, in the Beyer et al. (2018) test on natural xenoliths from the Jericho kimberlite, Slave craton, *P* estimates for eclogites were systematically lower (by ~1 GPa) than orthopyroxene–garnet *P* estimates for peridotites recording similar *T*. As a result, the Jericho eclogites oddly appeared to fall on a hotter geotherm. The *T*-dependence of the clinopyroxene–garnet barometer is ca. 0.25 GPa / 50 °C, i.e., similar to that of the orthopyroxene–garnet barometer. Therefore, also in this case, errors in input *T* would displace *P–T* estimates roughly along the geotherm and cannot explain the observed discrepancy between peridotite-system and eclogite-system thermobarometry results.

A further test of clinopyroxene–garnet thermobarometry is illustrated in Figure 5, for touching or non-touching inclusions in diamonds and diamond- or graphite-bearing xenoliths. The *P–T* estimates reflect iterations of the Beyer et al. (2015) barometer and the Nakamura (2009) Fe–Mg exchange thermometer. Since the uncertainty of the barometer increases rapidly with decreasing concentrations of $^{[4]}$Al in clinopyroxene, application to clinopyroxenes with Si contents >1.985 atoms per 6-oxygen formula is not recommended by Beyer et al. (2015). These compositions are relatively common for inclusions in diamonds (35% of 224 inclusions) and diamondiferous xenoliths (42% of 233 xenoliths), thus numerous samples had to be excluded. Even if further severe filters were applied to discard potentially low-quality chemical analyses, the results are disconcerting: although graphite-bearing xenoliths plot in the graphite stability field, most diamond-bearing xenoliths and inclusions in diamonds yield too low pressures

well outside the diamond stability field (Fig. 5). Iteration of earlier formulations of the same barometer and thermometer does not improve the results (cf. Fig. 10 in Shirey et al. 2013). The reason for this discrepancy is unclear. Simakov and Taylor (2000) cautioned that a barometer based on the Ca-Tschermak content in clinopyroxene may lead to incorrect estimates when applied to kyanite- or SiO_2-oversaturated assemblages, but the Beyer et al. (2015) barometer shows no systematic deviations in calculated pressures for experiments in these systems. The large chemical complexity of eclogitic garnets and, especially, eclogitic clinopyroxenes might in part explain the poor performance of the barometer in applications to natural systems, in which variable amounts of Na, Fe^{3+}, Cr, K and vacancy-bearing (i.e., Ca-Eskola) components occur. A further possible explanation is the high sensitivity of the barometer to even small errors in the chemical analyses of clinopyroxene. Beyer et al. (2015) provided a formula to predict relative errors on calculated pressures due to propagation of uncertainties on SiO_2 contents, assuming an uncertainty of 1% relative in electron microprobe analysis: $\%err = 1.94 \times 10^{-8} e^{10.18398[Si\ apfu]}$. These model errors do not consider the additional errors that derive from iterative calculation of *P* and *T* (Fig. 5). A 1% relative increase in SiO_2 contents may move many inaccurate *P*–*T* estimates into the diamond field, suggesting that application of the clinopyroxene–garnet barometer may require very high-quality, well-standardized electron microprobe analyses to yield meaningful results. Many of the analyses reported in the literature are possibly of routine quality and do not meet the necessary standards for robust clinopyroxene–garnet barometry. Still, analytical quality alone is unlikely to account for all of the observed discrepancies (Fig. 5).

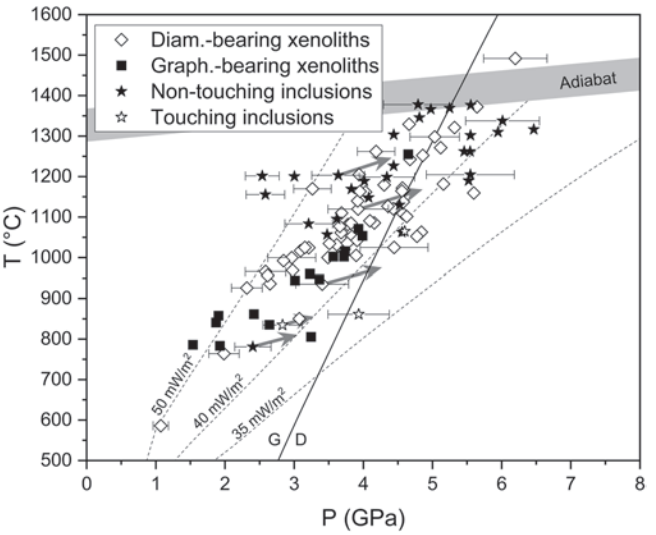

Figure 5. *P*–*T* estimates for diamond- or graphite-bearing eclogitic xenoliths and eclogitic clinopyroxene–garnet inclusion pairs in diamonds from worldwide sources, based on iteration of the Beyer et al. (2015) clinopyroxene–garnet barometer and Nakamura (2009) clinopyroxene–garnet thermometer. The following quality filters were adopted for clinopyroxenes: oxide totals = 99–101 wt%, cation totals per 6 oxygens = 3.99–4.02 apfu, Si < 1.985 apfu, X_{jd} < 0.5. The less restrictive upper limit for cation totals relative to the ideal value of 4 apfu allows for the presence of some Fe^{3+} in the clinopyroxene. These filters excluded 85% of 224 inclusions in diamonds and 73% of 233 diamond–eclogite xenoliths! Estimated *P* error bars based on Si contents (Beyer et al. 2015) are only shown for some representative samples. None of the data actually had errors smaller than the symbols. The grey arrows indicate the change in *P*–*T* estimates that is obtained by increasing the SiO_2 content in selected clinopyroxenes by 1% relative. Model-conductive geotherms for 35- and 40- and 50-mW/m^2 surface heat flow are after Hasterok and Chapman (2011). Mantle adiabat was calculated assuming a mantle potential temperature of 1327 ± 40 °C (Katsura et al. 2010). GD: graphite–diamond boundary after Day (2012).

Sun and Liang (2015) proposed that REE partitioning between clinopyroxene and garnet could be used not only as a thermometer (see above) but also as a barometer. Unfortunately, the discrepancies between calculated P_{REE} and run pressures for a set of independent validation experiments appear to be very large (up to ~3 GPa). A test conducted on twelve quartz eclogites, two graphite eclogites and nine diamond eclogites passed the appropriate stability-field constraints for all but two of the nine diamond eclogites; these fell at 0.2 and 0.5 GPa lower *P* than the diamond-graphite phase boundary. The proposed REE thermobarometry approach is promising, but further tests are necessary before this method can be used with confidence in diamond studies.

If trace element data are available, the partitioning of Li between clinopyroxene and garnet can also be used as a barometer (Hanrahan et al. 2009). Pressures for fifteen calibration experiments on a Mg-rich eclogitic composition at 4–13 GPa and 1100–1500 °C are reproduced to a very reasonable ±0.2 GPa (1 sigma) and the *T* dependence of the barometer is small (~0.2 GPa / 50 °C). Preliminary tests yielded conditions compatible with diamond for three diamond-bearing xenoliths and for non-touching inclusion pairs in four diamonds, whereas two other diamonds yielded conditions up to 2 GPa lower than the diamond stability field. Hanrahan et al. (2009) suggested that the two spurious *P* estimates could reflect disequilibrium between the non-touching inclusions. However, the use of non-touching inclusions is essential for this barometer, as the high diffusivity of Li may lead to reequilibration of small touching inclusions during and after transport to surface. Similar to the REE barometer, further tests are needed before this method can be recommended for diamond studies.

Monomineral barometers. Nimis and Taylor (2000) developed an empirical Cr-in-clinopyroxene barometer for chromian diopsides in equilibrium with garnet. In combination with the Nimis and Taylor (2000) single-clinopyroxene thermometer, this barometer uniquely permits derivation of both *P* and *T* conditions based on the composition of a single mineral inclusion. The *T*-dependence of the Cr-in-clinopyroxene barometer (0.15–0.25 GPa / 50 °C for diamond inclusion compositions) is generally lower than that of the orthopyroxene–garnet barometer (~0.2–0.3 GPa / 50 °C) and the *P*-dependence of the complementary single-clinopyroxene thermometer is very small (Fig. 4). Therefore, if *P* and *T* are calculated by iteration, errors in input *T* or *P* will displace a clinopyroxene *P*–*T* estimate at an angle relative to a cratonic geotherm and will contribute to 'apparent' scatter in *P*–*T* results for samples equilibrated on a steady-state geotherm. The Nimis and Taylor (2000) Cr-in-clinopyroxene barometer tends to progressively underestimate above 4.5 GPa (by up to ~1 GPa at 7 GPa; Nimis 2002; Ziberna et al. 2016). This is a known artifact and the discrepancy should be considered when comparing Cr-in-clinopyroxene estimates with those obtained using other methods. Nimis et al. (2020) proposed an empirical correction to minimize the differences with *P* estimates obtained using the orthopyroxene–garnet barometer at high *P*, at the cost of somewhat lower precision. These authors cautioned that their correction represented a temporary measure to reduce inconsistencies between independent barometric estimates. More recently, Sudholz et al. (2021b) provided an experimental recalibration of the Cr-in-clinopyroxene barometer that yields results very similar to the empirically corrected calibration for clinopyroxenes associated with diamonds or hosted in well equilibrated peridotitic xenoliths at $P > 5$ GPa (Fig. 6a). At lower *P* the two revised calibrations diverge slightly, but the Nimis et al. (2020) calibration maintains somewhat better overall consistency with orthopyroxene–garnet barometry (Fig. 6b,c). For proper application of the Cr-in-clinopyroxene barometer, the analyses must undergo compositional filtering in order to select clinopyroxenes in equilibrium with garnet and eliminate certain compositions for which analytical uncertainties propagate excessive uncertainties on the calculated *P*. Ziberna et al. (2016) provided a useful cookbook to perform the necessary compositional screening, which slightly improved an earlier one proposed by Grütter (2009). According to this cookbook, some compositions require that electron microprobe analyses are carried out using beam

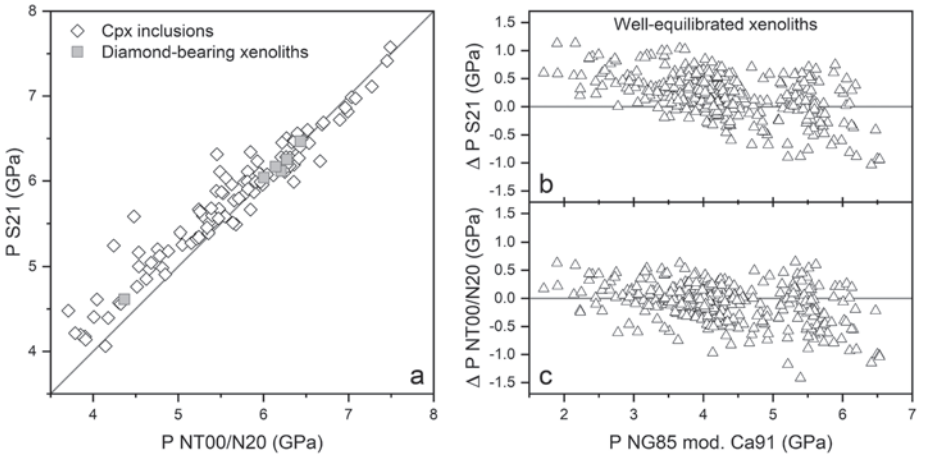

Figure 6. (a) Comparison between *P* estimates obtained with the Cr-in-clinopyroxene barometer, as recalibrated by Sudholz et al. (2021b) and Nimis et al. (2020), respectively, for clinopyroxenes included in diamonds and in diamond-bearing peridotitic xenoliths. (b-c) Deviations of *P* calculated with the Sudholz et al. (2021b) and Nimis et al. (2020) recalibrations of the Cr-in-clinopyroxene barometer from *P* estimated with the Nickel and Green (1985) orthopyroxene–garnet barometer for 349 well-equilibrated xenoliths (xenolith compilation after Nimis and Grütter 2010, with clinopyroxene compositions filtered according to Ziberna et al. 2016). For 87 xenoliths containing orthopyroxenes with Na > Cr + Ti (molar fractions), the Nickel and Green (1985) barometer was modified as suggested by Carswell (1991). The alternative modification proposed by Carswell and Gibb (1987) would produce somewhat lower *P* estimates for these samples and increased scatter at high *P* in both (b) and (c). All clinopyroxene pressures in (a), (b) and (c) were calculated by iteration with the Nimis and Taylor (2000) single-clinopyroxene thermometer. Orthopyroxene–garnet pressures in (b) and (c) were calculated by iteration with the Taylor (1998) two-pyroxene thermometer.

currents and counting times higher than routine to minimize analytical uncertainties, whereas some unfavorable compositions should simply be discarded. In particular, the recommended limitation to $Cr/(Cr+Al)_{mol} > 0.1$ excludes about two thirds of reported inclusions classified as websteritic. When applied to properly filtered graphite- or diamond-bearing xenoliths and inclusions in peridotitic diamonds, the Cr-in-clinopyroxene barometers yield results consistent with or within ~0.3 GPa of the stability field of the respective carbon phase (Nimis and Taylor 2000; see also Fig. 8a). The lack of adequate filtering in previously published thermobarometric results greatly contributed to the larger overall scatter in clinopyroxene *P–T* plots relative to those for orthopyroxene–garnet pairs (cf. Stachel and Harris 2008).

Griffin and Ryan (1995) devised an empirical barometer based on the Cr content of garnet in equilibrium with orthopyroxene and spinel. This Cr-in-garnet barometer was later refined by Ryan et al. (1996) and further revised, using a different Cr/Ca-in-garnet approach, by Grütter et al. (2006). The last two versions are the most widely used, typically in combination with a Ni-in-garnet thermometer. That of Grütter et al. (2006) gives up to ~10% lower estimates and a better agreement with petrological constraints imposed by the graphite–diamond transition, and is therefore preferable. If the coexistence of garnet with spinel is unknown, as is the case for many garnet inclusions in diamonds, the Cr-in-garnet methods only provide an estimate of minimum pressure.

Simakov (2008) proposed a simplified version of the clinopyroxene–garnet barometer for eclogites that solely relies on the Ca-Tschermak content in the clinopyroxene. The accuracy of this monomineral barometer cannot be better than that of the native two-phase barometer and is thus prone to the same problematic issues (see above). Ashchepkov et al. (2017) calibrated or recalibrated a series of empirical monomineral thermobarometers, which should be suitable

for peridotitic and eclogitic garnets and clinopyroxenes. When applied to mantle xenoliths and diamond inclusions from individual localities, these methods produce strongly scattered *P–T* estimates (e.g., Figs. 9–12 in Ashchepkov et al. 2017), which are difficult to compare with the more regular *P–T* distributions that are typically obtained with other, more widely tested methods. The usefulness of the Ashchepkov et al. (2017) monomineral formulations for diamond thermobarometry is therefore questionable.

With increasing pressure beyond ~7 GPa, mantle garnets incorporate increasing proportions of majoritic (i.e., pyroxene-like) component by substitution of Si for octahedrally coordinated Al and Cr. The Na and Ti contents also tend to increase. Collerson et al. (2000) utilized the relationship observed between majorite fractions and pressure in experiments on mafic and ultramafic systems to devise an empirical single-mineral barometer. The method was later revised by Collerson et al. (2010), Wijbrans et al. (2016) and Beyer and Frost (2017). Only Wijbrans et al. (2016) proposed two distinct calibrations, one for peridotitic and another for eclogitic systems. Experimental tests by Beyer and Frost (2017) and Beyer et al. (2018) showed systematic deviations or decreased precision for all but the Beyer and Frost (2017) formulation. This was particularly relevant for eclogitic compositions, which were underrepresented in previous calibration datasets. The Beyer and Frost (2017) barometer was calibrated at pressures of 6 to 20 GPa and temperatures of 900 to 2100 °C. These conditions cover sublithospheric mantle conditions up to ~575 km depth, corresponding to the lower transition zone. Experimental pressures are reproduced with a standard error of estimate of 0.86 GPa. In relative terms, considering the enormous range of pressures covered by the calibration, this uncertainty is not much larger than that of the barometers used for lithospheric diamonds. The effect of temperature on pressure estimates is apparently negligible. Note that application of the majorite barometer to lithospheric garnets equilibrated at $P < 6$ GPa is not recommended, because under such conditions the barometer becomes extremely sensitive to analytical errors (Beyer and Frost 2017). Tao et al. (2018) showed that high Fe^{3+} contents in the garnet tend to produce underestimated pressures with previous majorite barometers and provided a further revised calibration of the Collerson et al. (2010) barometer that explicitly takes into account Fe^{3+}. The Tao et al. (2018) calibration may be preferable when Fe^{3+} data are available and measured $Fe^{3+}/\Sigma Fe$ ratios are greater than 0.2. All these majorite barometers require that garnet occurs in equilibrium with a clinopyroxene phase. This may be an issue, because with increasing pressure pyroxene progressively dissolves into garnet and at pressures above ~15–19 GPa, depending on bulk composition and temperature, mantle rocks no longer contain pyroxene (Irifune et al. 1986; Irifune 1987; Okamoto and Maruyama 2004). Pyroxene-undersaturated condition can be suggested by the presence of $CaSiO_3$ phases along with majoritic garnet as inclusions in diamonds or by high Ca contents in majoritic garnet. Under such conditions, the barometer would give erroneously low pressures (Harte and Cayzer 2007). If there is no independent evidence that the garnet was pyroxene-saturated, any pressure estimates close to that of the clinopyroxene-out reaction should be considered as estimates of the minimum *P* of entrapment. Thomson et al. (2021) devised a novel type of majorite barometer using machine-learning algorithms. Compared to traditional majorite barometers, this new barometer is apparently insensitive to petrological limitations (most notably, the absence of clinopyroxene) and reproduces experimental majoritic garnet compositions over a wider range of bulk compositions and experimental pressures (6–25 GPa) with much better overall precision (mostly within ±2 GPa). Thomson et al. (2021) caution that the compositions of majoritic garnet inclusions in diamonds lie in a region with relatively fewer experiments and machine-learning regressions may not be reliable in extrapolation. Thus, pressure predictions for inclusions in diamonds may have somewhat larger uncertainties. Still, this is the only available barometric method that allows estimating pressures for majoritic garnet inclusions beyond the clinopyroxene-out reaction. When applied to inclusions in diamonds, differences between pressure estimates obtained with the Thomson et al. (2021) and Beyer and Frost (2017) barometers lie in the range –2.5 to +6 GPa. Whatever the majorite barometric

method used, if the garnet reequilibrated with clinopyroxene after entrapment, as is typically the case in unmixed inclusions (see below), underestimation of *P* will occur.

Elastic methods. When an inclusion is entrapped in a diamond, both the inclusion and the diamond are initially at the same pressure. On eruption, the pressure acting on the diamond drops to 1 atm, but a residual pressure, P_{inc}, of up to several GPa may develop on the inclusion as a consequence of the inclusion and host having different elastic properties. If we know the P_{inc} and the elastic properties of the inclusion and host, we can back-calculate the conditions under which the two minerals would be at the same pressure. These conditions describe a line in *P*–*T* space, known as the entrapment isomeke, and the entrapment conditions (i.e., the diamond formation *P*–*T*) will be one of the points along the isomeke. This forms the basis for elastic barometry of diamonds. The principles, problems and on-going developments of this method are described in detail in Angel et al. (2022, this volume).

Projection onto a geotherm. When only thermometric estimates are available due to a lack of suitable barometers, a tentative estimate of pressure can be obtained by projecting temperature estimates on a reference geotherm. This will most conveniently be a geotherm derived by fitting *P*–*T* data for mantle xenoliths or xenocrysts from the same kimberlitic source. The FITPLOT computational software by Mather et al. (2011) provides a useful aid to model geotherms from xenolith *P*–*T* data. There may be significant uncertainties in some of the input parameters that are used for the modeling, specifically the thickness and heat production of the upper and lower crust and the mantle potential temperature, but in most cases these uncertainties will not significantly affect the shape of the geotherm within the lithospheric diamond window, which will be chiefly constrained by the xenolith *P*–*T* data. Nonetheless, assuming different mantle potential temperatures will affect the estimated thickness of the lithosphere and the depth extent of the conductive portion of the geotherm. This may have some relevance for some old, high-*T* diamonds, as mantle potential temperatures may have varied over geological time. If this variation is not considered, thermometric estimates may unduly be projected onto the adiabatic portion of the geotherm and lead to severe overestimation of *P*. Values for the present-day mantle potential temperature and its change with time can be found in Katsura et al. (2010) and Ganne and Feng (2017). The output data that describe the relevant section of the model geotherm can conveniently be fitted through a polynomial expression to derive *P* as a function of *T*. The final *P*–*T* estimate will be given by the intersection of this polynomial with the isotherm described by the chosen thermometer. Note that this isotherm will not generally be a flat line in a *P*–*T* plot, due to the generally significant *P*-dependence of the thermometers (Fig. 4).

The basic assumption underlying this approach is that the inclusions last equilibrated at *P*–*T* conditions lying on the mantle geotherm at the time of eruption. This is generally acceptable for touching inclusion pairs, which can reequilibrate in mostly the same way as touching minerals in xenoliths (but see caveat in section below dedicated to touching vs. non-touching inclusions), whereas it is much less obviously so for non-touching inclusions. Comparisons between *P*–*T* estimates for inclusions and xenoliths from the same sources showed that the assumption often holds also for non-touching inclusions (Nimis 2002). Nonetheless, there is also evidence of some diamond inclusions recording conditions significantly hotter or colder than the xenolith geotherm (Griffin et al. 1993; Sobolev and Yefimova 1998; Nimis 2002; Stachel et al. 2003, 2004; Weiss et al. 2018; Nimis et al. 2020). Also, multiple non-touching inclusions within individual diamonds may record a range of conditions, indicating thermal fluctuations during the growth history of the diamond (Griffin et al. 1993). Projection onto a geotherm should therefore be used with caution and relatively large uncertainties should be allowed. Assuming a maximum possible *T* difference from a xenolith geotherm of ~250 °C, consistent with available estimates for diamonds using single-clinopyroxene (Nimis and Taylor 2000), single-garnet (Canil 1999) and orthopyroxene–garnet (Harley 1984) thermometers, projection on a typical cratonic geotherm may result in a *P* uncertainty of up to ~1.5 GPa (Fig. 4).

Projection onto the adiabatic portion of the mantle geotherm may provide a necessary independent constraint for the application of elastic barometric methods to sublithospheric diamonds (e.g., Anzolini et al. 2019).

Mineral stability. Lithospheric mantle rocks provide little opportunity to estimate conditions of diamond formation based only on the stability of mineral assemblages. For example, across the entire diamond window, the only significant mineralogical change is the spinel-to-garnet transition in peridotite. The spinel-to-garnet reaction is not univariant and in depleted cratonic peridotites with strongly elevated Cr/Al, spinel + garnet assemblages may persist over a large range of *P–T* conditions (e.g., MacGregor 1970; Webb and Wood 1986; Klemme 2004; Ziberna et al. 2013). In general, spinel is stabilized to higher pressures in more refractory, Cr-rich and Al-poor bulk compositions. This allows magnesiochromite to be incorporated as inclusions in diamonds that were formed in very deep, refractory environments (e.g., 6.5 GPa, corresponding to a depth of over 200 km, for a diamond from the Udachnaya kimberlite, Siberia; Nestola et al. 2019a).

Mineral stabilities become more interesting in the sublithospheric mantle, where a number of characteristic mineralogical changes occur (Harte 2010; Harte and Hudson 2013). Although these changes do not permit bracketing of *P–T* conditions with a resolution comparable to that of conventional thermobarometers, in some cases they constrain the formation of a diamond to within specific mantle depth regions. For instance, the coexistence of Fe-bearing periclase with enstatite, interpreted to be inverted bridgmanite (previously known as MgSi-perovskite), has long provided evidence that some diamonds were formed at lower-mantle depths (Scott Smith et al. 1984; Moore et al. 1986). Even in the absence of periclase, inverted bridgmanite from the lower mantle can readily be distinguished from upper-mantle enstatite by its very low Ni contents (Stachel et al. 2000). The finding of a rare inclusion of ringwoodite in a diamond from Juina, Brazil, unequivocally demonstrated its origin from the mantle transition zone (Pearson et al. 2014). Also, the reconstructed compositions of a suite of exsolved inclusions in Juina diamonds nicely matched those of minerals expected to form in a basaltic system in the lower mantle (Walter et al. 2011).

However, using incomplete mineral assemblages found as inclusions in diamonds as depth markers is not always free from ambiguity. For instance, inclusions of breyite (previously known as CaSi-walstromite) have long been considered to represent retrogressed $CaSiO_3$-perovskite from depths greater than ~600 km (e.g., Harte et al. 1999; Joswig et al. 1999), but there is compelling evidence that at least some breyite inclusions originated at much shallower depths within the upper mantle (Brenker et al. 2005; Anzolini et al. 2016). Woodland et al. (2020) recently provided experimental support for a possible upper-mantle origin of breyite. Also, Fe-bearing periclase is the most common inclusion of interpreted lower-mantle origin (Kaminsky 2012), but there is evidence that Fe-bearing periclase participates in mineral parageneses straddling the upper mantle-lower mantle boundary (Hutchison et al. 2001) and that it may be a co-product of diamond-forming reactions that may occur in the transition zone and even in the overlying upper mantle (Thomson et al. 2016; Bulatov et al. 2019).

Best practices in diamond thermobarometry

Data quality. A sometimes underrated prerequisite for robust thermobarometry is precise and accurate chemical analyses. Inclusions in diamonds are often small and their chemical analysis can be challenging. Moreover, some thermobarometers may be particularly sensitive to analytical uncertainties on elements that occur at critical concentration levels. For instance, Ziberna et al. (2016) explored propagation of analytical errors on *P* estimates using the single-clinopyroxene barometer of Nimis and Taylor (2000) and found that routine electron microprobe analytical conditions may be insufficient for meaningful barometry of many inclusions in diamonds. Clearly, not only poor counting statistics but also bad sample

preparation and improper standardization can be an issue and may lead to spurious results. A survey of published chemical data for over 600 clinopyroxene inclusions in lithospheric diamonds reveals that ~30% of them have oxide total weight percentages <98.5% or >101%, or cation sums < 3.98 or > 4.03 atoms per formula unit and, thus, are definitely not of good quality! Note that the above cut-offs generously take into account the possible effects of considering all Fe as Fe^{2+} in electron microprobe analyses.

The next critical step when studying inclusions that were separated from coexisting mineral phases is the definition of their original paragenesis. Even if single-mineral thermobarometers may often come in handy, they invariably assume that the investigated mineral last equilibrated with specific other minerals. As for clinopyroxene and garnet, which are major constituents in several types of mantle rocks, simple compositional screening based on either major or trace element concentrations may help to discriminate between the most typical paragenetic varieties (e.g., Griffin et al. 2002; Grütter et al. 2004; Nimis et al. 2009; Ziberna et al. 2016). Unusual compositions that are not sensitively discriminated by available classification schemes or fall outside the compositional range over which the thermobarometers were calibrated, as well as false positives that unduly survive compositional filtering, may undermine the reliability of thermobarometric data. This problem may be minimized by investigating large datasets, when this is permitted by the number and nature of the available samples.

Even when all cautionary steps have been made to select suitable compositional data, thermobarometric estimates are subject to errors. As discussed in the previous section, some of these errors are systematic and lead to predictable inconsistencies between estimates obtained using different methods. This fact should always be considered when comparing data obtained using different thermobarometers or even different formulations of the same thermobarometer. Thermobarometric methods with demonstrated internal consistency must be prioritized if the purpose is to explore the distribution of data for heterogeneous inclusion populations.

In this respect, thermobarometry of eclogitic diamonds remains problematic. Considering the compositional limitations required by the 'best' available barometric methods (i.e., $Si_{Cpx} < 1.985$ apfu and $Na_{Cpx} < 0.5$ apfu), ~45% of over 200 reported eclogitic clinopyroxene–garnet inclusion pairs are automatically excluded. In addition, the reliability of barometric methods for eclogitic inclusions is questionable (see above).

When *P* estimates are too uncertain or not available, for example, due to a lack of suitable barometers for the specific inclusions investigated, projection of temperatures onto the local xenolith geotherm can provide a last-resort solution to estimate *P*. The resulting uncertainties can be too large for an accurate characterization of genesis conditions for individual diamonds, but the procedure can have some utility for exploring general trends in large datasets (e.g., Korolev et al. 2018; Nimis et al. 2020). It probably remains the safest available method for barometry of eclogitic inclusions, notwithstanding potential over- or underestimation for diamonds formed at conditions hotter or, respectively, colder than ambient mantle at the time of eruption. A fairly popular alternate has been to calculate *T* for these diamonds at a fixed *P* of 5 GPa, approximately corresponding to the average *P* for diamonds worldwide. This method is not as effective and may overcompress the range of *T* estimates, due to the generally significant *P*-dependence of the thermometers (Fig. 4).

Touching vs. non-touching. When a pair of touching mineral grains included in a diamond reequilibrate to changing external conditions, their total encapsulated volume remains constrained by the surrounding diamond. This forces the included minerals to follow a distinct pressure path and to achieve final compositions that are different from those of the same minerals outside the diamond (see Angel et al. 2015 and Ferrero and Angel 2018 for more general discussion of this phenomenon). The most common changes in ambient conditions are probably isobaric cooling or heating after diamond growth, in response to secular variations

in mantle thermal state or following short-term thermal pulses related to diamond-forming processes. In most cases of diamond-hosted inclusions, cooling will cause a decrease in the inclusion *P* even if the external *P* remains constant, leading to underestimation of the actual diamond *P* using chemical thermobarometers. The extent of this underestimation can be calculated if the thermoelastic properties of the inclusion and host minerals are known (Angel et al. 2015). For various combinations of garnet, pyroxene and olivine inclusions in diamond, the error would amount to ~0.3 GPa for a temperature drop of 100 °C. Heating will have the opposite effect. These errors are of a similar magnitude as those of the orthopyroxene–garnet and single-clinopyroxene barometers and may thus contribute to some of the scatter in *P–T* plots for touching inclusions. The resulting errors may be lower, however, if plastic deformation in the diamond is able to reduce the under- or overpressures developed on the inclusions.

If some thermal reequilibration occurs, the use of single-mineral thermobarometers on touching inclusions may generate further errors when some key minerals are not part of the inclusion assemblage. For instance, touching inclusions of clinopyroxene-orthopyroxene devoid of garnet will reliably record the ambient thermal state at the time of eruption, but will be poor candidates for single-clinopyroxene barometry. In response to a thermal change, the clinopyroxene will easily reequilibrate with orthopyroxene, but not with garnet, and so a false apparent encapsulation *P* will be calculated at the final equilibrium *T* (Nimis 2002). Touching inclusions of clinopyroxene ± garnet ± olivine would instead produce estimates close to the diamond formation conditions, because the composition of the clinopyroxene in orthopyroxene-free assemblages would be little affected by a variation in temperature. Polymineralic inclusions consisting of touching clinopyroxene-orthopyroxene–garnet ± olivine will fully reequilibrate and will provide *P and T* conditions close to those at the time of eruption (except for the small systematic errors described in the previous paragraph).

Non-touching inclusions are immune to the above problems, because the inert diamond protects them from post-entrapment reequilibration, and are unequivocally the best candidates to determine the diamond formation *P–T*, provided reliable monomineral thermobarometers can be used. In all other cases, non-touching inclusion pairs are prone to potential errors, because the individual inclusions may have been incorporated at different times and under different conditions (see above) and may thus not be in mutual equilibrium. The largest *T* difference between multiple inclusions in individual diamonds was reported for garnets in a diamond from the Mir kimberlite, Siberia (Griffin et al. 1993). The calculated difference varies greatly depending on which calibration of the Ni-in-garnet thermometer is used, i.e., ca. 400 °C with the Ryan et al. (1996) calibration or ca. 230 °C with the Canil (1999) calibration. Disequilibrium amongst non-touching inclusions in diamonds, however, appears to be the exception rather than the rule, as multiple inclusions in individual diamonds most often yield similar *P–T* estimates once the systematic deviations between different thermobarometers are taken into account (Stachel and Harris 2008; Stachel and Luth 2015).

Syngenesis vs. protogenesis. For several decades, thermobarometry of inclusions in diamonds has relied on the assumption of syngenesis, i.e., the inclusions formed or completely recrystallized during the growth of diamond. A corollary of this assumption was that the inclusions record the conditions of diamond formation, excepting for potential post-entrapment modifications in touching inclusions. The main proof for syngenesis was that diamond typically imposed its shape on the inclusions. This widely accepted paradigm was challenged by Nestola et al. (2014), who found evidence of protogenesis (i.e., formation before the diamond) for some olivine inclusions that would have been classified as syngenetic based on morphological criteria. Similar evidence was then found for other olivine, clinopyroxene, garnet and magnesiochromite inclusions (Milani et al. 2016; Nestola et al. 2017, 2019b; Nimis et al. 2019). The possibility that inclusions in diamonds are protogenetic suggests that they might record conditions predating diamond formation. This might be particularly relevant for isolated inclusions, if their host

diamonds were formed from hot fluids or melts intruding through relatively cool mantle rocks. Did the preexisting mineral grains have enough time to fully reequilibrate to the changing thermal conditions during diamond growth and before their incorporation was complete?

The time required by a mineral to adjust its composition to new physicochemical conditions strongly depends on temperature and grain size, and can be estimated from diffusion kinetics. For instance, a clinopyroxene grain with a diameter of 200 μm would fully reset its Ca/Mg ratio (the main temperature sensor in pyroxene thermometry) in less than 100,000 yr above 1200 °C and in a few m.y. below 900 °C (Fig. 7). Whether these time spans are short or long enough for complete reequilibration depends on the diamond growth rate, which is not precisely known. It is tempting to infer that incomplete reequilibration of protogenetic inclusions, especially the largest and shallowest (i.e., coldest) ones, may account for some of the scatter in *P–T* plots for non-touching inclusions (Fig. 8). Also, the similarity of *P–T* conditions occasionally observed for inclusions in diamonds and xenoliths from the same sources may alternatively be ascribed to diamond formation from thermally-equilibrated media (Nimis 2002) or to lack of reequilibration of protogenetic inclusions during short-lived diamond-forming processes (Nestola et al. 2014).

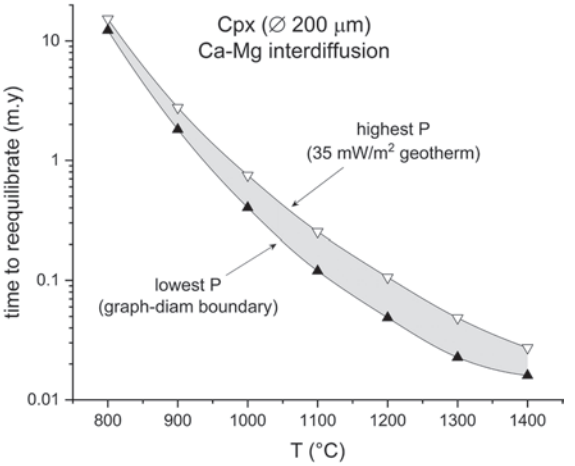

Figure 7. Time required to reequilibrate the Ca/Mg ratio in a spherical clinopyroxene grain with diameter of 200 μm as a function of temperature. The two curves are calculated from Ca-Mg inter-diffusion data (Zhang et al. 2010) for compositions on the pyroxene solvus at pressures corresponding to a 35 mW/m^2 geotherm (≈ maximum *P* for lithospheric diamonds) and to the graphite–diamond boundary (minimum *P* for diamonds), respectively. Increasing or decreasing the grain diameter by a factor of 2 would increase or, respectively, decrease the reequilibration time by a factor of ~4.

Exsolved inclusions. Some inclusions in diamonds show evidence of post-entrapment unmixing. Reported examples are clinopyroxenes with orthopyroxene exsolution lamellae (± coesite), representing unmixed high-*T* clinopyroxenes, and intergrowths of more or less majoritic garnet and clinopyroxene, representing unmixed high-*P* majoritic garnets.

Exsolved clinopyroxene inclusions are uncommon and have only been reported in diamonds from Namibian placers and from the Voorspoed kimberlite, South Africa (Leost et al. 2003; Viljoen et al. 2018). The coexistence of clinopyroxene and orthopyroxene makes these inclusions ideal for pyroxene thermometry, but the exsolved assemblage does not provide barometric estimates. Since pyroxene thermometers have a small *P*-dependence, projection onto the local xenolith geotherm provides in these cases reasonable estimates of the depth of

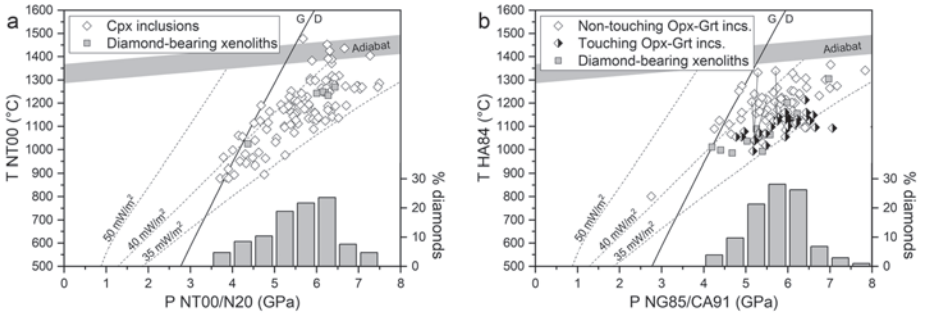

Figure 8. (**a**) *P–T* estimates for chromian clinopyroxene inclusions in worldwide diamonds (n = 100) and diamond-bearing lherzolitic xenoliths (n = 6) calculated with the Nimis and Taylor (2000) single-clinopyroxene barometer (as corrected by Nimis et al. 2020) and thermometer. Using the Sudholz et al. (2021b) recalibration of the clinopyroxene barometer would have produced broadly similar results (cf. Fig. 6). All compositions were filtered as recommended by Ziberna et al. (2016). Twenty-six (retained) compositions would have required better than routine EMPA counting statistics to minimize *P* uncertainties, but insufficient analytical details were provided. These records did not produce any particular deviations from the overall or local trends and therefore were not discarded. The great majority of the inclusions were isolated within the diamonds. Inclusions of clinopyroxene in contact with orthopyroxene but not with garnet were not considered, because post-entrapment reequilibration in these inclusions may produce spurious barometric results (Nimis 2002). (**b**) *P–T* estimates for orthopyroxene–garnet inclusion pairs in worldwide diamonds (n = 92) and diamond-bearing xenoliths (n = 11) calculated with a combination of the Harley (1984) thermometer and Nickel and Green (1985) barometer, with the modification to the barometer introduced by Carswell (1991) for orthopyroxenes with Na > Cr + Ti (molar fractions). Six orthopyroxene analyses with cation sums <3.98 atoms per formula unit were not considered. The compositions of multiple inclusions in individual diamonds were averaged, so that any single *P-T* point corresponds to one diamond. Tie lines in (b) connect touching inclusions in diamonds from Mwadui, Jwaneng and Jagersfontein with non-touching inclusions in other diamonds from the same localities and similar depths. Some of the apparent discrepancies between the two plots can be ascribed to known systematic inconsistencies between the thermobarometers used (see text for further explanation). Conductive geotherms for 35- and 40- and 50-mW/m^2 surface heat flow after Hasterok and Chapman (2011). The mantle adiabat was calculated assuming a mantle potential temperature of 1327 ± 40 °C (Katsura et al. 2010). GD: graphite–diamond boundary after Day (2012). Sources of data for diamond inclusions and diamondiferous xenoliths used in the plots: Aulbach (1999), Boyd (1984), Boyd and Finnerty (1980), Creighton et al. (2008), Daniels and Gurney (1989), Davies et al. (2004a,b), Dawson and Smith (1975), De Stefano et al. (2009), Deines and Harris (2004), Geological Survey of Canada (1989), Gurney et al. (1984), Harris et al. (1994, 2004, and unpubl.), Hervig et al. (1986), Hutchison (1997), Jaques et al. (1989, 1990), Kopylova et al. (1997), Korolev et al. (2018), Logvinova et al. (2015), McDade and Harris (1999), Moore and Gurney (1989), Nimis et al. (2020), Otter and Gurney (1989), Phillips et al. (2004), Pokhilenko et al. (1977, 2004), Ponomarenko et al. (1980), Rickard et al. (1989), Shee et al. (1982), Sobolev (1977), Sobolev et al. (1976, 1997a,b, 1999, 2009), Stachel and Harris (1997a,b), Stachel et al. (1998, 2003, 2004, 2018), Tappert et al. (2005, 2006), Tsai et al. (1979), University of Cape Town (unpubl. reports), Van Rythoven and Schulze (2009), Van Rythoven et al. (2011), Viljoen et al. (1992), Wang et al. (2000), Wilding et al. (1994).

origin of the diamonds (Nimis et al. 2020). If the compositions and relative proportions of the exsolved phases are known (e.g., by combining electron microprobe data with 2D or, better, 3D image analyses), the integrated pre-exsolution composition of the clinopyroxene can be reconstructed. The integrated composition can provide a *T* estimate at the time of diamond growth, assuming equilibrium with a separate orthopyroxene during entrapment, or a minimum *T* estimate of diamond formation, in the absence of orthopyroxene. In the reported cases, thermometry of the reconstructed clinopyroxenes provided evidence for diamond formation at temperatures near the mantle adiabat and ~200 °C hotter than the ambient mantle at the time of eruption. Attempts to apply the single-clinopyroxene barometer to the reconstructed compositions yielded unreasonably low pressure estimates, suggesting formation in strongly modified mantle environments (Nimis et al. 2020).

Exsolution textures are common in majoritic garnet inclusions in sublithospheric diamonds (Moore and Gurney 1989; Wilding 1990; Harte and Cayzer 2007). These textures are interpreted to reflect decompression during slow ascent of the diamonds in convecting mantle or mantle plumes. The presence of exsolutions implies that pressure estimates based on majoritic garnet compositions are minima. Using reconstructed pre-exsolution garnet compositions will yield conditions closer to those of diamond formation. Even so, the resulting estimates may be minima, because the garnet may have originated at depths beyond the clinopyroxene-out reaction (see previous Barometry section).

P–T DATA FOR DIAMONDS

Lithospheric diamonds

Figure 8 shows a compilation of *P–T* data for lithospheric diamonds from worldwide sources, obtained using the most robust available thermobarometer combinations. The compilation comprises clinopyroxene inclusions in 100 lherzolitic diamonds and orthopyroxene–garnet inclusion pairs in 77 harzburgitic, 12 lherzolitic and 10 websteritic diamonds. The great majority of the clinopyroxene inclusions were isolated within their host diamonds and should generally record conditions close to those of diamond formation. The orthopyroxene–garnet pairs consist of both touching and non-touching assemblages. The touching pairs may have reequilibrated after their incorporation and should provide conditions close to the final conditions of residence in the mantle. In addition, *P–T* data were calculated, using the same methods, for diamondiferous xenoliths for which suitable mineral analyses were available.

In comparing the two plots for single-clinopyroxene and orthopyroxene–garnet thermobarometry (Fig. 8a,b), it is important to consider the known systematic inconsistencies between the thermobarometric methods used (see above). The orthopyroxene–garnet thermometer tends to overestimate temperature below 1100 °C and to underestimate above 1100 °C. This accounts at least in part for the more restricted temperature range obtained for the orthopyroxene–garnet inclusions. Nonetheless, disregarding a single obvious outlier, all *P–T* values fall within 0.3 GPa of the diamond stability field, confirming the general reliability of the thermobarometers. Most of the *P–T* results lie between the 35- and 40-mW/m^2 conductive geotherms of Hasterok and Chapman (2011), i.e., at conditions typical for cratonic lithospheres. Most exceptions record higher temperature conditions, which in the case of clinopyroxene may reach the mantle adiabat. All of these exceptions consist of non-touching inclusions. A possible explanation is that several diamonds were formed from thermally non-equilibrated media derived from the sublithospheric convective mantle. Another potential source of mantle temperature inhomogeneity during diamond formation can be incomplete cratonization at the time of diamond growth. For instance, in the Kaapvaal craton a stable geothermal gradient was established by about 2.5 Ga and followed by secular cooling (e.g., Michaut and Jaupart 2007; Brey and Shu 2018) and re-heating (Griffin et al. 2003), but many Kaapvaal diamonds are significantly older than 2.5 Ga (see review in Shirey and Richardson 2011) or may have formed during important perturbations of the local lithosphere (Griffin et al. 2003; Korolev et al. 2018). Therefore, it is not surprising that many of these diamonds may record conditions hotter or colder than those at the time of kimberlite eruption (e.g., Nimis et al. 2020).

The touching orthopyroxene–garnet inclusion pairs deserve further discussion. In the available dataset, the majority of them (23 out of 31) refer to diamonds from the De Beers Pool (Kimberley, South Africa). These inclusions were studied by Phillips et al. (2004), who carefully documented differences between *P–T* estimates recorded by touching vs. non-touching inclusions. These workers found that the non-touching inclusions yielded higher *P–T* values than the touching inclusions and ascribed this observation to post-entrapment reequilibration of the touching inclusions under decreasing *T* conditions, possibly accompanied by mantle

uplift and decompression. They also correctly noted that post-entrapment elastic modifications were not of sufficient magnitude to reconcile the observed *P–T* differences between touching and non-touching inclusions. However, Nimis et al. (2020) observed that both touching and non-touching inclusions in the Phillips et al. (2004) dataset record a colder geothermal regime than mantle xenoliths and xenocrysts in the same kimberlites, casting doubts on the secular cooling hypothesis. Whereas the relatively cold signature of the non-touching inclusions might reflect old conditions pre-dating the final thermal equilibration of the lithosphere recorded by the xenoliths, the data for the touching inclusions are difficult to interpret. Weiss et al. (2018) speculated that the low temperatures recorded by the touching inclusions could be related to late infiltration of cold, slab-derived fluids, remnants of which were preserved in some cloudy and coated diamonds from the same locality. Yet it remains unclear why infiltration of these fluids should leave virtually no traces in the sampled mantle xenoliths.

Touching orthopyroxene–garnet inclusions from other localities are probably too few to be statistically significant. Nonetheless, in all these cases the touching inclusions yield temperatures significantly lower than non-touching inclusions in other diamonds from about the same depth (Fig. 8b). Additional thermobarometric evidence that diamond formation may be followed by cooling was provided by Stachel and Luth (2015) and Viljoen et al. (2018). However, Stachel and Luth (2015) also described touching inclusions yielding temperatures similar to or even slightly higher (up to 40 °C) than non-touching inclusions in the same diamonds.

Diamond's depth systematics. Irrespective of the nature of the inclusions and the thermobarometric methods used, the frequency distribution of pressures for lithospheric diamond is essentially unimodal, with a mode at ~6 GPa, corresponding to depths around ~190 km (Fig. 8; see also Stachel and Harris 2008 and Stachel 2014 for broadly similar distributions obtained using different thermobarometers and partly different datasets). The slight differences between the pressure distributions obtained for clinopyroxene and orthopyroxene–garnet inclusions may largely be ascribed to recognized inconsistencies between the different thermobarometer combinations used and, perhaps, to sampling bias. Therefore, these differences are probably not significant. The hard constraints imposed by the graphite–diamond and lithosphere-asthenosphere boundaries cannot fully explain the observed depth distributions, which show decreased diamond frequencies approaching these boundaries (Fig. 8). Nimis et al. (2020) obtained very similar depth distributions with depth modes at 180 ± 10 km for diamonds from three individual South African kimberlite sources by using various combinations of thermobarometric methods on different inclusion types. They also found no clear correlation with the depth distributions of mantle xenocrysts from the same sources calculated using the same thermobarometric methods. They concluded that the observed diamond depth distributions are unrelated to the kimberlite sampling efficiency and, thus, have genetic meaning and likely global significance.

The global significance of the observed depth distributions is also supported by the abundant $T_{\text{Ni-in-garnet}}$ data for garnet inclusions (Fig. 9). These data show a mode at ~1200 °C, but no pressure constraints are generally available. Assuming that the garnets last equilibrated at 'average' conditions between the 35- and 40- mW/m^2 model geotherms, similar to the clinopyroxene and orthopyroxene–garnet inclusions (Fig. 8), the Ni-in-garnet temperature mode would correspond, again, to a pressure mode of ~6 GPa and a depth mode of ~190 km. The gentler increase of frequencies to ~1200 °C and their steeper decrease at higher temperatures (Fig. 9) also mirror the frequency variations with increasing pressure to ~6 GPa and beyond exhibited by the clinopyroxene and orthopyroxene–garnet inclusions (Fig. 8).

The diamond depth distributions in the lithosphere may be the result of both constructive and destructive processes (Nimis et al. 2020). In particular, the progressive decrease in diamond concentrations at depths shallower than ~170–190 km may reflect (i) decreasing precipitation rates for diamond from ascending parental media or (ii) progressive decrease

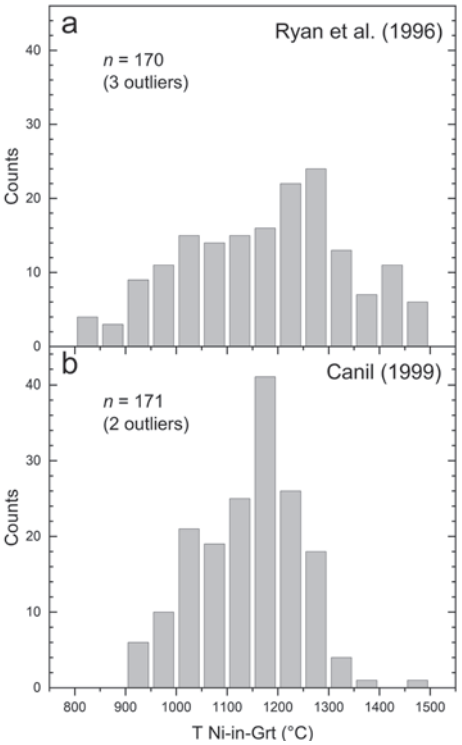

Figure 9. Frequency distribution of Ni-in-Grt temperatures for garnet inclusions in diamonds, assuming 2900 ppm Ni in olivine and using the Ryan et al. (1996) and Canil (1999) calibrations. The distribution shows a distinct mode at ~1175 °C for the Canil (1999) calibration and a less distinct mode at ~1250 °C for the Ryan et al. (1996) calibration. Sources of inclusion data as in Fig. 1.

in the amount of these deep-sourced media at shallower levels. Probably, both mechanisms concur to limit the diamond endowment in the shallow portion of the diamond window. The rapid decrease of diamonds near the base of the lithosphere may reflect (i) a positive balance between the opposed effects that an increase of *P* and an increase of *T* may have on carbon solubility in some mantle fluids/melts along specific *P–T* paths or (ii) a progressive decrease in diamond endowment due to reactions with carbon-undersaturated asthenospheric fluids/melts. These two alternative hypotheses are difficult to prove or disprove, because our knowledge of the behavior of natural carbon-bearing melts and fluids at high *P–T* is still limited. The prevalence of melt-metasomatized lithologies near the base of typical lithospheres coincides with diminished diamond frequency and suggests that melt-driven metasomatism may be an important destructive agent for diamond (e.g., McCammon et al. 2001). Remobilization of carbon from these deep lithospheric roots may eventually contribute to build up the diamond concentration at shallower depths (Nimis et al. 2020).

The recognition that depths around ~190 km are particularly favorable for diamonds may have interesting implications for their mineralogical exploration. Areas characterized by the occurrence of xenocrystic mantle minerals (e.g., clinopyroxenes or garnets) from these particular depths may be considered as high-priority targets. Nonetheless, since the xenocrysts and diamond depth distributions may be uncorrelated, even limited xenocryst records from the diamond's most favorable depth range may be indicative of significant diamond potential (Nimis et al. 2020).

Sublithospheric diamonds

Figure 10 shows the global distribution of pressure estimates for diamonds containing majoritic garnets. At present, these are the only types of inclusions that provide abundant, quantitative barometric data for sublithospheric diamonds. A difficulty in investigating these data lies in the fact that they may represent minimum *P* estimates. As explained in the previous section, this limitation is due to the frequent occurrence of exsolutions and, for all but the Thomson et al. (2021) barometer, to the possible absence of accompanying clinopyroxene in the original mineral assemblage from which the majoritic garnet inclusion was separated on entrapment. If one considers only inclusions that are reportedly free of clinopyroxene exsolutions, two distinct unimodal distributions are obtained for peridotitic and eclogitic/pyroxenitic garnets, respectively (Fig. 10). Using the Beyer and Frost (2017) barometer, the peridotitic inclusions are mostly clustered in the 175–225 and 225–275 km depth intervals, near the lithosphere-asthenosphere boundary. Most of these inclusions would thus more appropriately be classified as deep lithospheric. The eclogitic/pyroxenitic inclusions are, on average, much deeper and mostly fall in the depth interval between 300 and 500 km. If one considers also inclusions that do contain exsolved pyroxenes, the peak of eclogitic/pyroxenitic inclusions at ~400 km becomes more prominent. Using the Thomson et al. (2021) barometer, the distribution for the eclogitic/pyroxenitic inclusions is stretched to slightly higher pressures, with a maximum estimated depth of 613 ± 44 km, whereas many of the peridotitic inclusions are shifted to significantly greater depths, falling well into the sublithospheric region (Fig. 10). Some of the deepest (>450 km) majoritic garnets fall in the region where clinopyroxene disappears and thus the Beyer and Frost (2017) barometer may underestimate pressure for these samples. However, the Thomson et al. (2021) machine-learning barometer, which is immune to this effect, does not suggest a much deeper origin for these garnets (Fig. 10). Differences between depth estimates for these very deep samples using the two alternative barometers are between –65 and +81 km (average +17 km).

It should be considered that, in some cases, in the absence of accurate imaging data, the occurrence of fine clinopyroxene exsolutions may have been overlooked. The use of improved BSE and EBSD imaging might allow recognition of exsolved clinopyroxene in nominally 'clinopyroxene-free' majoritic inclusions (cf. Harte and Cayzer 2007; Zedgenizov et al. 2014). The thirteen Juina majoritic inclusions for which no coexisting clinopyroxene has been reported to date give depth estimates in a restricted range between 353 and 455 km (using the Beyer and Frost 2017 barometer) or 368 to 462 km (using the Thomson et al. 2021 barometer) and are in part responsible for the prominent peak at ~400 km in Figure 10. If these inclusions also contained exsolutions and the available electron microprobe data do not faithfully reflect their original compositions, then the overall peak could be shifted to somewhat greater depths or, at least, the overall depth distribution would be smoother than shown in Figure 10. Thomson et al. (2021) suggested that all majoritic garnet inclusions in South American diamonds probably contain exsolutions. They also noted that in the eight inclusions for which both exsolved and reconstructed bulk compositions were available the amount of exsolution is a simple function of the calculated pressure. Accordingly, they devised an empirical correction that can be applied to all inclusions for which reconstructed bulk compositions are not available. When this correction is applied to South American diamonds, the peak for eclogitic majoritic garnet inclusions is smoothed and shifted to ca. 100 km greater depth. It remains unclear if this correction, which is based on a restricted number of inclusions, has any general validity at either global or local scale. In any case, the high abundance of depth estimates between ~300 and ~500 km, even for inclusions that are certainly clinopyroxene-free or whose original composition was reconstructed, suggests that most of the eclogitic/pyroxenitic majoritic garnets indeed originated from this depth range (Harte 2010), or perhaps from a slightly more extended range of ~300 to ~600 km if the Thomson et al. (2021) correction for South

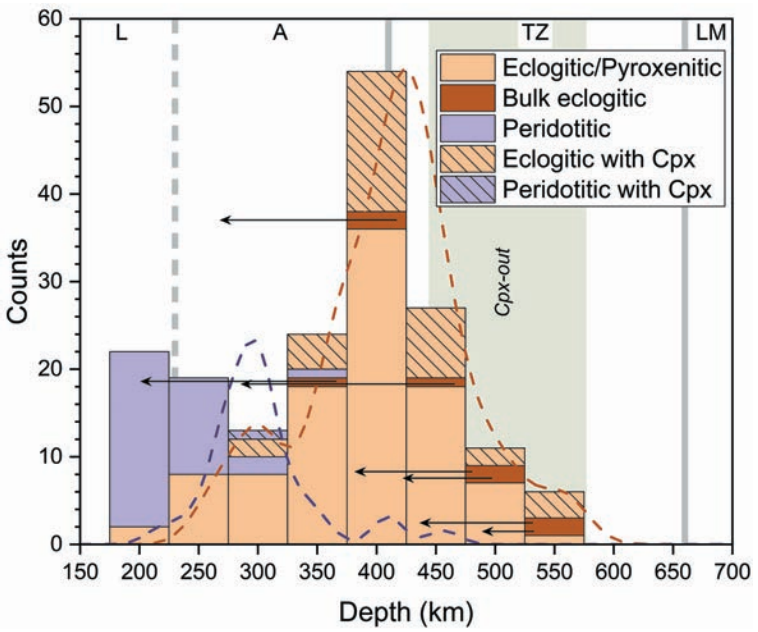

Figure 10. Distribution of estimated depths for inclusions of majoritic garnet (Si > 3.05 atoms per formula unit) in worldwide diamonds, based on barometric estimates (Beyer and Frost 2017) and using the Preliminary Reference Earth Model (PREM; Dziewonski and Anderson 1981) for pressure-depth conversion. 'Bulk' refers to exsolved eclogitic inclusions for which the original pre-exsolution composition was reconstructed; **arrows** connect their depth estimates with those obtained using the compositions of the respective exsolved garnets, where available. Other inclusions in which garnet was reported to be in contact with clinopyroxene or probably contained fine clinopyroxene exsolutions are shown separately, as these garnets certainly reequilibrated to lower pressure conditions during their long journey to the surface. The **dashed curves** show the kernel density distribution of depths for the same eclogitic (**brown**) and peridotitic (**purple**) samples obtained using the machine-learning barometer of Thomson et al. (2021). The **shaded green** area corresponds to the depth range over which clinopyroxene disappears in different bulk compositions (Irifune et al. 1986; Irifune 1987; Okamoto and Maruyama 2004); depth estimates falling within this area using the Beyer and Frost (2017) barometer may be underestimated (see text for further explanation). L: lithosphere. A: asthenosphere. TZ: transition zone. LM: lower mantle. Sources of data: Bulanova et al. (2010), Burnham et al. (2015, 2016), Davies et al. (1999, 2004b), Deines et al. (1991), Harte and Caizer (2007), Hutchison (1997), Kaminsky et al. (2001), Korolev et al. (2018), Meyer and Mahin (1986), Meyer et al. (1994), Moore and Gurney (1985, 1989), Moore et al. (1991), Motsamai et al. (2018), Pokhilenko et al. (2004), Schulze et al. (2008), Shatskii et al. (2010), Shatsky et al. (2015), Smith et al. (2009, 2016), Sobolev et al. (1997b, 2004), Stachel and Harris (1997b), Stachel et al. (2000, 2006), Tappert et al. (2005), Thomson et al. (2014, 2021), Tsai et al. (1979), University of Cape Town (unpubl. reports), Wilding (1990), Zedgenizov et al. (2014).

American diamonds is valid. This range overlaps with independent depth estimates obtained from phase stability constraints for other sublithospheric diamonds containing Ca-silicate inclusions (300–360 km; Brenker et al. 2005; Anzolini et al. 2016) and with a minimum depth estimate obtained from elastic barometry for a single ferropericlase inclusion (~450 km; Anzolini et al. 2019). Of further interest, the 300–600 km range corresponds to the depths at which carbonated MORB slabs are most likely to intersect their solidus, providing an ideal environment for focused melting and potential diamond growth (Thomson et al. 2016, 2021). Considering that many periclase-magnesiowüstite inclusions, for which barometric data are not available, may also have formed from subduction-related melts (Thomson et al. 2016; Nimis et al. 2018) the actual proportion of diamonds from the 300–600 km interval may be even larger than shown in Figure 10. The reader is referred to Walter et al. (2022, this volume) for a thorough discussion on these and related aspects.

A second favorable region for diamond formation is probably located near the upper mantle–lower mantle boundary and uppermost lower mantle (Harte 2010). Evidence for diamond formation in this region is provided by a number of key mineral associations within individual diamonds, mostly consisting of various combinations of periclase, $(Mg,Fe)SiO_3$, $(Mg,Fe)_2SiO_4$, jeffbenite (formerly known as TAPP), breyite, corundum and SiO_2, and of a NaAl-pyroxene phase (believed to have formed as highly majoritic garnet) alongside with periclase or jeffbenite (Hutchison et al. 2001; Harte 2010). Although in several diamonds only part of the key mineral assemblages is actually represented, the general consistency between the observed mineral associations led Harte (2010) to suppose that a large number of diamonds could come from the relatively narrow depth range of 600 to 800 km. Most inclusions in diamonds from this depth range are ultramafic, as opposed to the mafic inclusions that dominate in the 300–600 km interval.

CONCLUSIONS AND FUTURE WORK

Mineral inclusions are very rare in diamonds and occur in only about 1% of examined stones, with significant differences between individual localities (Stachel and Harris 2008). Moreover, only a few mantle minerals or mineral assemblages that may occur as inclusions in diamonds are suitable for thermobarometry. Therefore, only a small proportion of natural diamonds may yield robust information on the *P–T* conditions of their formation, and these diamonds are mostly peridotitic. This proportion may increase in the future, in parallel with the development of new thermobarometric methods or refinement of existing ones. A significant field of potential and desirable improvement concerns the eclogitic inclusions, which represent a major fraction of inclusions in lithospheric diamonds, but for which existing barometric methods still provide inconsistent results. A dedicated test on clinopyroxene–garnet pairs similar to that performed on chromian diopsides by Ziberna et al. (2016) might shed more light on the minimum analytical quality that is required for reliable barometry of these inclusions. Extending the applicability of non-traditional methods, such as elastic barometry, to non-ideal configurations and to a more diverse list of inclusion minerals might also have a dramatic effect on the number of diamonds suitable for thermobarometry, although the need for elastically preserved inclusions generally restricts applications to relatively small inclusions not surrounded by fractures. An interesting advantage of the elastic method is that it can rely on non-destructive techniques and, thus, can leave the samples intact and ready for further investigation with other methods. Such investigations require the use of undamaged samples in which internal strains are well preserved. Legacy destructive techniques used to expose minerals included in diamond, unfortunately, prohibit future examination of these unique samples for purposes of elastic barometry.

Reanalysis of some previously investigated inclusions or diamondiferous xenoliths might provide a relatively effortless way to increase the number of diamond *P–T* data. Four of 195 published chromian clinopyroxene analyses and 6 of 156 published orthopyroxene analyses had to be discarded while preparing this review only because of sub-standard analytical quality. Moreover, twenty-five clinopyroxenes were rejected because their compositions fell just off the major-element compositional fields that are used to classify garnet-associated chromian diopsides (Ziberna et al. 2016). Trace element analysis of these diopsides might have allowed more robust discrimination (e.g., based on Sc/V relationships; Nimis et al. 2009) of the garnet-associated samples and many of them might have turned out to be suitable for thermobarometry. Reintegrating all these samples would increase the number of *P–T* data for chromian diopside-bearing diamonds by a remarkable 27% and for diamonds overall by 17%.

An enlargement of the number of *P–T* data for diamonds would have significant positive outcomes in terms of sample bias reduction. Sample bias is presently a major problem, since

the number of localities for which a statistically significant number of sufficiently reliable *P–T* estimates are currently available is limited at best to three and all are from the Kaapvaal craton (Nimis et al. 2020). Consequent benefits of sample bias reduction would be a better assessment of diamond depth distributions at individual localities, and a more robust evaluation of diamond *P–T* systematics and of their significance in terms of diamond forming processes and preservation.

If the number of *P–T* data for diamonds is important, their internal consistency may be even more so. In fact, most of the combinations of thermobarometric methods that may be applied to diamond inclusions do show some degree of inconsistency with one another. These inconsistencies mostly stem from simplified thermodynamic treatment of solid solutions in minerals and from uncertainties in the data used for their calibration and derived either from experiments or from independent xenolith thermobarometry. The internal consistency of thermobarometric methods is particularly critical when comparing data for different inclusion types, as commonly is necessary in diamond studies. This is another field of potential scientific advance that may eventually contribute to an improved understanding of diamond forming processes.

ACKNOWLEDGMENTS

This review is the result of the knowledge, expertise and generosity of many people. Fruitful collaboration through the years with many of them, and particularly with W.R. Taylor, H. Grütter, L. Ziberna, F. Nestola and R.J. Angel, has been of decisive importance in producing my personal contributions to diamond thermobarometry. Yet many more people have in fact contributed to this review through their enormous scientific work and by providing the community with invaluable data over about five decades. Most of them appear in the reference list below. I express my sincere gratefulness to all of these people and, in particular, to T. Stachel, who generously shared a diamond inclusion database, which served as a useful basis to build the updated database used in this work. I am also grateful to A. Thomson, for help in majorite barometry calculations, and to H. Grütter, G. Brey and editor T. Stachel for their very helpful and thorough reviews and comments.

REFERENCES

Angel RJ, Nimis P, Mazzucchelli ML, Alvaro M, Nestola F (2015) How large are departures from lithostatic pressure? Constraints from host-inclusion elasticity. J Metamorph Geol 33:801–813

Angel RJ, Alvaro M, Nestola F (2022) Crystallographic methods for non-destructive characterization of mineral inclusions in diamonds. Rev Mineral Geochem 88:257–306

Anzolini C, Angel RJ, Merlini M, Derzsi M, Tokár K, Milani S, Krebs MY, Brenker FE, Nestola F, Harris JW (2016) Depth of formation of $CaSiO_3$-walstromite included in super-deep diamonds. Lithos, 265:138–147

Anzolini C, Nestola F, Mazzucchelli M, Alvaro M, Nimis P, Gianese A, Morganti S, Marone F, Campione M, Hutchison MT, Harris J (2019) Depth of diamond formation obtained from single periclase inclusions. Geology 47:219–222

Ashchepkov IV, Pokhilenko NP, Vladykin NV, Logvinova AM, Kostrovitsky SI, Afanasiev VP, Pokhilenko LN, Kuligin SS, Malygina LV, Alymova NV, Khmelnikova OS, Palessky SV, Nikolaeva IV, Karpenko MA, Stagnitsky YB (2010) Structure and evolution of the lithospheric mantle beneath Siberian craton, thermobarometric study. Tectonophysics 485:17–41

Ashchepkov IV, Ntaflos T, Logvinova AM, Spetsius ZV, Downes H, Vladykin NV (2017) Monomineral universal clinopyroxene and garnet barometers for peridotitic, eclogitic and basaltic systems. Geosci Frontiers 8:775–795

Aulbach S (1999) The chemistry of syngenetic mineral inclusions in diamonds from Venetia and the stable isotope composition of diamonds from Mwadui and the Kankan district. MSc Thesis, JW Goethe University, Frankfurt, Germany

Batanova VG, Sobolev AV, Magnin V (2018) Trace element analysis by EPMA in geosciences: detection limit, precision and accuracy. IOP Conf Series: Mater Sci Eng 304:012001

Beyer C, Frost DJ (2017) The depth of sub-lithospheric diamond formation and the redistribution of carbon in the deep mantle. Earth Planet Sci Lett 461:30–39

Beyer C, Frost DJ, Miyajima N (2015) Experimental calibration of a garnet–clinopyroxene geobarometer for mantle eclogites. Contrib Mineral Petrol 169:1–21

Beyer C, Rosenthal A, Myhill R, Crichton WA, Yu T, Wang Y, Frost DJ (2018) An internally consistent pressure calibration of geobarometers applicable to the Earth's upper mantle using in situ XRD. Geochim Cosmochim Acta 222:421–435

Boyd FR (1984) Siberian geotherm based on lherzolite xenoliths from the Udachnaya kimberlite, U.S.S.R. Geol 12:528–530

Boyd FR, Finnerty AA (1980) Conditions of origin of natural diamonds of peridotite affinity. J Geophys Res 85:6911–6918

Brenker FE, Vincze L, Vekemans B, Nasdala L, Stachel T, Vollmer C, Kersten M, Somogyi A, Adams F, Joswig W (2005) Detection of a Ca-rich lithology in the Earth's deep (>300 km) convecting mantle. Earth Planet Sci Lett 236:579–587

Brey GP, Köhler T (1990) Geothermobarometry in four-phase lherzolites. II. New thermobarometers, and practical assessment of existing thermobarometers. J Petrol 31:1353–1378

Brey GP, Shu Q (2018) The birth, growth and ageing of the Kaapvaal subcratonic mantle. Mineral Petrol 112:23–41

Bulanova G, Walter M, Smith C, Kohn S, Armstrong L, Blundy J, Gobbo L (2010) Mineral inclusions in sublithospheric diamonds from Collier 4 kimberlite pipe, Juina, Brazil: subducted protoliths, carbonated melts and primary kimberlite magmatism: Contrib Mineral Petrol 160:489–510

Bulatov VK, Girnis AV, Brey GP, Woodland AB, Höfer HE (2019) Ferropericlase crystallization under upper mantle conditions, Contrib Mineral Petrol. 174:45

Burnham AD, Thomson AR, Bulanova GP, Kohn SC, Smith CB, Walter MJ (2015) Stable isotope evidence for crustal recycling as recorded by superdeep diamonds. Earth Planet Sci Lett 432:374–380

Burnham AD, Bulanova GP, Smith CB, Whitehead SC, Kohn SC, Gobbo L, Walter MJ (2016) Diamonds from the Machado River alluvial deposit, Rondônia, Brazil, derived from both lithospheric and sublithospheric mantle. Lithos 265:199–213

Bussweiler Y, Brey GP, Pearson DG, Stachel T, Stern RA, Hardman MF, Kjarsgaard BA, Jackson SE (2017) The aluminum-in-olivine thermometer for mantle peridotites experimental versus empirical calibration and potential applications. Lithos 272–273:301–314

Canil D (1999) The Ni-in-garnet geothermometer: calibration at natural abundances. Contrib Mineral Petrol 136:240–246

Carswell DA (1991) The garnet–orthopyroxene Al barometer: problematic application to natural garnet lherzolite assemblages. Mineral Mag 55:19–31

Carswell DA, Gibb FG (1987) Evaluation of mineral thermometers and barometers applicable to garnet lherzolite assemblages. Contrib Mineral Petrol 95:499–511

Collerson KD, Hapugoda S, Kamber BS, Williams Q (2000) Rocks from the mantle transition zone: majorite-bearing xenoliths from Malaita, southwest Pacific. Science 288:1215–1223

Collerson KD, Williams Q, Kamber BS, Omori S, Arai H, Ohtani E (2010) Majoritic garnet: a new approach to pressure estimation of shock events in meteorites and the encapsulation of sub-lithospheric inclusions in diamond. Geochim Cosmochim Acta 74:5939–5957

Creighton S (2009) A semi-empirical manganese-in-garnet single crystal thermometer. Lithos 112S:177–182

Creighton S, Stachel T, McLean H, Muehlenbachs K, Simonetti A, Eichenberg D, Luth R (2008) Diamondiferous peridotitic microxenoliths from the Diavik Diamond Mine, NT. Contrib Mineral Petrol 155:541–554

Czas J, Pearson DG, Stachel T, Kjarsgaard BA, Read GH (2020) A Palaeoproterozoic diamond-bearing lithospheric mantle root beneath the Archean Sask Craton, Canada. Lithos 356–357:105301

Daniels LRM, Gurney JJ (1989) The chemistry of garnets, chromites and diamond inclusions from the Dokolwayo kimberlite, Kingdom of Swaziland. *In*: Kimberlites and Related Rocks. Ross J et al. (eds) GSA Spec Publ 14. Blackwell, Carlton, p 1012–1021

Davies RM, Griffin WL, Pearson NJ, Andrew AS, Doyle BJ, O'Reilly SY (1999) Diamonds from the deep: pipe DO-27, Slave craton, Canada. *In*: The J.B. Dawson Volume, Proc VIIth Int Kimberlite Conf. Gurney JJ, Gurney JL, Pascoe MD, Richardson SH (eds) Red Roof Design, Cape Town, p 148–155

Davies RM, Griffin WL, O'Reilly SY, Doyle BJ (2004a) Mineral inclusions and geochemical characteristics of microdiamonds from the DO27, A154, A21, A418, DO18, DD17 and Ranch Lake kimberlites at Lac de Gras, Slave Craton, Canada. Lithos 77:39–55

Davies RM, Griffin WL, O'Reilly SY, McCandless TE (2004b) Inclusions in diamonds from the K14 and K10 kimberlites, Buffalo Hills, Alberta, Canada: diamond growth in a plume? Lithos 77:99–111

Dawson JBM, Smith JV (1975) Occurrence of diamond in a mica–garnet lherzolite xenolith from kimberlite. Nature 254:580–581

Day HW (2012) A revised diamond–graphite transition curve. Am Mineral 97:52–62

De Hoog JCM, Gall L, Cornell DH (2010) Trace-element geochemistry of mantle olivine and application to mantle petrogenesis and geothermobarometry. Chem Geol 270:196–215

De Hoog JCM, Stachel T, Harris JW (2019) Trace-element geochemistry of diamond-hosted olivine inclusions from the Akwatia Mine, West African Craton: implications for diamond paragenesis and geothermobarometry. Contrib Mineral Petrol 174:100

Deines P, Harris JW, Gurney JJ (1991) The carbon isotopic composition and nitrogen content of lithospheric and asthenospheric diamonds from the Jagersfontein and Koffiefontein kimberlite, South Africa. Geochim Cosmochim Acta 55:2615–2625

Deines P, Harris JW (2004) New insights into the occurrence of ^{13}C-depleted carbon in the mantle from two closely associated kimberlites: Letlhakane and Orapa, Botswana. Lithos 77:125–142
De Stefano A, Kopylova MG, Cartigny P, Afanasiev V (2009) Diamonds and eclogites of the Jericho kimberlite (Northern Canada). Contrib Mineral Petrol 158:295–315
D'Souza RJ, Canil D, Coogan LA (2020) Geobarometry for spinel peridotites using Ca and Al in olivine. Contrib Mineral Petrol 175:5
Dziewonski AM, Anderson DL (1981) Preliminary reference Earth model. Phys Earth Planet Inter 25:297–356
Ferrero S, Angel RJ (2018) Micropetrology: are inclusions grains of truth? J Petrol 59:1671–1700
Ganne J, Feng X (2017) Primary magmas and mantle temperatures through time. Geochem Geophys Geosyst 18:872–888
Geological Survey of Canada (1989) The development of advanced technology to distinguish between diamondiferous and barren diatremes. Open File 2124
Griffin WL, Ryan CG (1995) Trace elements in indicator minerals: area selection and target evaluation in diamond exploration. J Geochem Expl 53:311–337
Griffin WL, Gurney JJ, Ryan CG (1992) Variations in trapping temperatures and trace elements in peridotite-suite inclusions from African diamonds: evidence for two inclusion suites, and implications for lithosphere stratigraphy. Contrib Mineral Petrol 110:1–15
Griffin WL, Sobolev NV, Ryan CG, Pokhilenko NP, Win TT, Yefimova ES (1993) Trace elements in garnets and chromites: diamond formation in the Siberian lithosphere. Lithos 29:235–256
Griffin WL, Fisher NI, Friedman JH, O'Reilly SY, Ryan CG (2002) Cr-pyrope garnets in the lithospheric mantle: 2. Compositional populations and their distribution in time and space. Geochem Geophys Geosyst 3:1073
Griffin WL, O'Reilly SY, Natapov LM, Ryan CG (2003) The evolution of lithospheric mantle beneath the Kalahari Craton and its margins. Lithos 71:215–241
Grütter HS (2009) Pyroxene xenocryst geotherms: Techniques and application. Lithos 112S:1167–1178
Grütter H, Apter DB, Kong J (1999) Crust–mantle coupling: evidence from mantle-derived xenocrystic garnets. *In*: The J.B. Dawson Volume, Proc VIIth Int Kimberlite Conf. Gurney JJ, Gurney JL, Pascoe MD, Richardson SH (eds), Red Roof Design, Cape Town, p. 307–313
Grütter HS, Gurney JJ, Menzies AH, Winter F (2004) An updated classification scheme for mantle-derived garnet, for use by diamond explorers. Lithos 77:841–857
Grütter H, Latti D, Menzies A (2006) Cr-saturation arrays in concentrate garnet compositions from kimberlite and their use in mantle barometry. J Petrol 47:801–820
Grütter HS, Tuer J (2009) Constraints on deep mantle tenor of Sarfartoq-area kimberlites (Greenland), based on modern thermobarometry of mantle-derived xenocrysts. Lithos 112S, 124–129
Gurney JJ, Harris JW, Rickard RS (1984) Minerals associated with diamonds from the Roberts Victor Mine. *In*: Kimberlites II: The Mantle and Crust-Mantle Relationships. Kornprobst J (ed) Elsevier, Amsterdam, p 25–32
Hanrahan H, Brey G, Woodland A, Seitz H-M, Ludwig T (2009) Li as a barometer for bimineralic eclogites: Experiments in natural systems. Lithos 112S:992–1001
Harley SL (1984) An experimental study of the partitioning of Fe and Mg between garnet and orthopyroxene. Contrib Mineral Petrol 86:359–373
Harris JW, Duncan DJ, Zhang F, Mia Q, Zhu Y (1994) The physical characteristics and syngenetic inclusion geochemistry of diamonds from pipe 50, Liaoning Province, People's Republic of China. *In*: Diamonds: Characterization, Genesis and Exploration. Meyer HOA, Leonardos OH (eds) CPRM Spec Publ Jan/94, Brasilia, p 106–115
Harris JW, Stachel T, Leost I, Brey GP (2004) Peridotitic diamonds from Namibia: constraints on the composition and evolution of their mantle source. Lithos 77:209–223
Harte B (2010) Diamond formation in the deep mantle: the record of mineral inclusions and their distribution in relation to mantle dehydration zones. Mineral Mag 74:189–215
Harte B, Cayzer N (2007) Decompression and unmixing of crystals included in diamonds from the mantle transition zone. Phys Chem Minerals 34:647–656
Harte B, Hudson NFC (2013) Mineral associations in diamonds from the lowermost upper mantle and uppermost lower mantle. *In*: Proc 10th Int Kimb Conf. Vol 1. Pearson DG et al. (eds) Spec Issue J Geol Soc India, p 235–253
Harte B, Harris J, Hutchison M, Watt G, Wilding M (1999) Lower mantle mineral associations in diamonds from São Luiz, Brazil. *In*: Mantle Petrology: Field Observations and High-Pressure Experimentation: A tribute to Francis R. (Joe) Boyd. Fei Y, Bertka CM, Mysen BO (eds) Geochem Soc Spec Publ No 6, p 125–153
Hasterok D, Chapman DS (2011) Heat production and geotherms for the continental lithosphere. Earth Planet Sci Lett 307:59–70
Hervig RL Smith JV and Dawson JB (1986) Lherzolite xenoliths in kimberlites and basalts: petrogenetic and crystallographic significance of some minor and trace elements in olivine, pyroxenes, garnet and spinel. Trans R Soc Edin Earth Sci 77:181–201
Hutchison MT (1997) Constitution of the deep transition zone and lower mantle shown by diamonds and their inclusions. PhD Thesis, University of Edinburgh, Scotland, UK
Hutchison MT, Hursthouse MB, Light ME (2001) Mineral inclusions in diamonds: Associations and chemical distinctions around the 670-km discontinuity. Contrib Mineral Petrol 142:119–126
Irifune T (1987) An experimental investigation of the pyroxene-garnet transformation in a pyrolite composition and its bearing on the constitution of the mantle. Phys Earth Planet Inter 45:324–336

Irifune T, Ringwood AE, Hibberson WO (1986) The eclogite–garnetite transformation at high pressure and some geophysical implications. Earth Planet Sci Lett 77:245–256

Jaques AL, Hall AE, Sheraton JW, Smith CB, Sun S-S, Drew RM, Foudoulis C, Ellingsen K (1989) Composition of crystalline inclusions and C-isotopic composition of Argyle and Ellendale diamonds. *In*: Kimberlites and Related Rocks. Ross J et al. (eds) Geol Soc Australia Spec Publ Spec Publ 14. Blackwell, Carlton, p 966–989

Jaques AL, O'Neill HStC, Smith CB, Moon J, Chappell BW (1990) Diamondiferous peridotite xenoliths from the Argyle (AK1) lamproite pipe, Western Australia. Contrib Mineral Petrol 104:255–276

Joswig W, Stachel T, Harris JW, Baur WH, Brey GP (1999) New Ca-silicate inclusions in diamonds – tracers from the lower mantle. Earth Planet Sci Lett 173:1–6

Kaminsky FV (2012) Mineralogy of the lower mantle: A review of 'super-deep' mineral inclusions in diamond. Earth-Sci Rev 110:127–147

Kaminsky FV, Zakharchenko OD, Davies R, Griffin WL, Khachatryan-Blinova GK, Shiryaev AA (2001) Superdeep diamonds from the Juina area, Mato Grosso State, Brazil. Contrib Mineral Petrol 140:734–753

Katsura T, Yoneda A, Yamazaki D, Yoshino T, Ito E (2010) Adiabatic temperature profile in the mantle. Phys Earth Planet Int 183:212–218

Klemme S (2004) The influence of Cr on the garnet–spinel transition in the Earth's mantle: experiments in the system $MgO–Cr_2O_3–SiO_2$ and thermodynamic modelling. Lithos 77:639–646

Kohn SC, Speich L, Smith CB, Bulanova GP (2016) FTIR thermochronometry of natural diamonds: a closer look. Lithos 265:148–158

Kopylova MG, Gurney JJ, Daniels LRM (1997) Mineral inclusions in diamonds from the River Ranch kimberlite, Zimbabwe. Contrib Mineral Petrol 129:366–384

Korolev NM, Kopylova M, Bussweiler Y, Pearson DG, Gurney J, Davidson J (2018) The uniquely high-temperature character of Cullinan diamonds: A signature of the Bushveld mantle plume? Lithos 304–307:362–373

Krogh EJ (1988) The garnet–clinopyroxene Fe–Mg-geothermometer—a reinterpretation of existing experimental data. Contrib Miner Pet 99:44–48

Leost I, Stachel T, Brey GP, Harris JW, Ryabchikov ID (2003) Diamond formation and source carbonation: mineral associations in diamonds from Namibia. Contrib Mineral Petrol 145:15–24

Logvinova AM, Taylor LA, Fedorova EN, Yelisseyev AP, Wirth R, Howarth G, Reutsky VN, Sobolev NV (2015) A unique diamondiferous peridotite xenolith from the Udachnaya kimberlite pipe, Yakutia: role of subduction in diamond formation. Russ Geol Geophys 56:306–320

MacGregor ID (1970) The effect of CaO, Cr_2O_3, Fe_2O_3 and Al_2O_3 on the stability of spinel and garnet peridotites. Phys Earth Planet Inter 3:372–377

MacGregor ID (1974) The system MgO-$A1_2O_3$-SiO_2: solubility of $A1_2O_3$ in enstatite for spinel and garnet peridotite compositions. Am Mineral 59:110–119

Malkovets VG, Zedgenizov DA, Sobolev NV, Kuzmin DV, Gibsher AA, Shchukina EV, Golovin NN, Verichev EM, Pokhilenko NP (2011) Contents of trace elements in olivines from diamonds and peridotite xenoliths of the V. Grib kimberlite pipe (Arkhangel'sk Diamondiferous Province, Russia). Dokl Earth Sci 436:219–223

Mather KA, Pearson DG, McKenzie D, Kjarsgaard BA, Priestley K (2011) Constraints on the depth and thermal history of cratonic lithosphere from peridotite xenoliths, xenocrysts and seismology. Lithos 125:729–742

Matjuschkin V, Brey GP, Höfer HE, Woodland AB (2014) The influence of Fe^{3+} on garnet–orthopyroxene and garnet–olivine geothermometers. Contrib Mineral Petrol 167:972

McCammon CA, Griffin WL, Shee SR, O'Neill HSC (2001) Oxidation during metasomatism in ultramafic xenoliths from the Wesselton kimberlite, South Africa: implications for the survival of diamond. Contrib Mineral Petrol 141:287– 296

McDade P, Harris JW (1999) Syngenetic inclusion bearing diamonds from Letseng-la-Terai, Lesotho. *In*: The P.H. Nixon Volume, Proc VIIth Int Kimberlite Conf. Gurney JJ, Gurney JL, Pascoe MD, Richardson SH (eds) Red Roof Design, Cape Town, p 557–565

Mendelssohn MJ, Milledge HJ (1995) Geologically significant information from routine analysis of the mid-infrared spectra of diamonds. Int Geol Rev 37:95–110

Meyer HOA, Mahin RA (1986) The kimberlites of Guinea, West Africa. 4th Int Kimberlite Conf Abstr, Geol Soc Aus Abstr Series 16:66

Meyer HOA, Zhang A, Milledge HJ, Mendelssohn MJ (1994) Diamonds and inclusions in diamonds from Chinese kimberlites. *In*: Proc 5th Int Kimberlite Conf, vol 1, Diamonds: characterization, genesis and exploration. Meyer HOA, Leonardos OH (eds) CPRM, Brasilia, p 98–105

Michaut C, Jaupart C (2007) Secular cooling and thermal structure of continental lithosphere. Earth Planet Sci Lett 257:83–96

Milani S, Nestola F, Angel RJ, Nimis P, Harris JW (2016) Crystallographic orientations of olivine inclusions in diamonds. Lithos 265:312–316

Moore RO, Gurney JJ (1985) Pyroxene solid solution in garnets included in diamond. Nature 318:553–555

Moore RO, Gurney JJ (1989) Mineral inclusions in diamond from the Monastery kimberlite, South Africa. *In*: Kimberlites and Related Rocks. Vol 2. Their Mantle/Crust Setting, Diamonds and Diamond Exploration, Proc 4th Int Kimberlite Conf. Ross J et al. (eds) Geol Soc Aust Spec Publ 14:1029–1041

Moore RO, Otter ML, Rickard RS, Harris JW, Gurney JJ (1986) The occurrence of moissanite and ferro-periclase as inclusions in diamond. 4th Int Kimberlite Conf Ext Abstr, Perth. Geol Soc Aust Abstr, 16:409–411

Moore RO, Gurney JJ, Griffin WL, Shimizu N (1991) Ultra-high pressure garnet inclusions in Monastery diamonds: trace element abundance patterns and conditions of origin. Eur J Mineral 3:213–230

Motsamai T, Harris JW, Stachel T, Pearson DG, Armstrong J (2018) Mineral inclusions in diamonds from Karowe Mine, Botswana: Super-deep sources for super-sized diamonds? Miner Petrol 112:169–180

Nakamura D (2009) A new formulation of garnet–clinopyroxene geothermometer based on accumulation and statistical analysis of a large experimental data set. J Metamorph Geol 27:495–508

Nestola F, Nimis P, Angel RJ, Milani S, Bruno M, Prencipe M, Harris JW (2014) Olivine with diamond-imposed morphology included in diamonds. Syngenesis or protogenesis? Int Geol Rev 56:1658-1667

Nestola F, Haemyeong J, Taylor LA (2017) Mineral inclusions in diamonds may be synchronous but not syngenetic. Nat Commun 8:14168

Nestola F, Zaffiro G, Mazzucchelli ML, Nimis P, Andreozzi GB, Periotto B, Princivalle F, Lenaz D, Secco L, Pasqualetto L, Logvinova AM, Sobolev NV, Lorenzetti A, Harris JW (2019a) Diamond-inclusion system recording old deep lithosphere conditions at Udachnaya (Siberia). Sci Rep 9:12586

Nestola F, Jacob DE, Pamato MG, Pasqualetto L, Oliveira B, Greene S, Perritt S, Chinn I, Milani S, Kueter N, Sgreva N, Nimis P, Secco L, Harris JW (2019b) Protogenetic garnet inclusions and the age of diamonds. Geology 47:431–434

Nickel KG, Green DH (1985) Empirical geothermobarometry for garnet peridotites and implications for the nature of the lithosphere, kimberlites and diamonds. Earth Planet Sci Lett 73:158–170

Nimis P (2002) The pressures and temperatures of formation of diamond based on thermobarometry of chromian diopside inclusions. Can Mineral 40:871–884

Nimis P, Grütter H (2010) Internally consistent geothermometers for garnet peridotites and pyroxenites. Contrib Mineral Petrol 159:411–427

Nimis P, Taylor WR (2000) Single clinopyroxene thermobarometry for garnet peridotites; Part I, Calibration and testing of a Cr-in-Cpx barometer an enstatite-in-Cpx thermometer. Contrib Mineral Petrol 139:541–554

Nimis P, Zanetti A, Dencker I, Sobolev NV (2009) Major and trace element composition of chromian diopsides from the Zagadochnaya kimberlite (Yakutia, Russia): Metasomatic processes, thermobarometry and diamond potential. Lithos 112:397–412

Nimis P, Goncharov A, Ionov DA, McCammon C (2015) Fe^{3+} partitioning systematics between orthopyroxene and garnet in mantle peridotite xenoliths and implications for thermobarometry of oxidized and reduced mantle rocks. Contrib Mineral Petrol 169:6

Nimis P, Nestola F, Schiazza M, Reali R, Agrosì G, Mele D, Tempesta G, Howell D, Hutchison M, Spiess R (2018) Fe-rich ferropericlase and magnesiowüstite inclusions reflecting diamond formation rather than ambient mantle. Geology 47:27–30

Nimis P, Angel RJ, Alvaro M, Nestola F, Harris JW, Casati N, Marone F (2019) Crystallographic orientations of magnesiochromite inclusions in diamonds: What do they tell us? Contrib Mineral Petrol 174:29

Nimis P, Preston R, Perritt SH, Chinn IL (2020) Diamond's depth distribution systematics. Lithos 376–377:105729

Okamoto K, Maruyama S (2004) The eclogite–garnetite transformation in the MORB + H_2O system. Phys Earth Planet Inter 146:283–296

O'Neill HStC, Wood BJ (1979) An experimental study of Fe–Mg partitioning between garnet and olivine and its calibration as a geothermometer. Contrib Mineral Petrol 70:59–70

O'Reilly SY, Chen D, Griffin WL, Ryan CG (1997) Minor elements in olivine from spinel lherzolite xenoliths: implications for thermobarometry. Mineral Mag 61:257–269

Otter ML, Gurney JJ (1989) Mineral inclusions in diamond from the Sloan diatremes, Colorado-Wyoming State Line kimberlite district, North America. *In*: Kimberlites and Related Rocks. Ross J et al. (eds) Geol Soc Australia Spec Publ Spec Publ 14. Blackwell, Carlton, p 1042–1053

Pearson D, Brenker F, Nestola F, McNeill J, Nasdala L, Hutchison M, Matveev S, Mather K, Silversmit G, Schmitz S, (2014) Hydrous mantle transition zone indicated by ringwoodite included within diamond. Nature 507:221–224

Phillips D, Harris JW, Viljoen KS (2004) Mineral chemistry and thermobarometry of inclusions from De Beers Pool diamonds, Kimberley, South Africa. Lithos 77:155–179

Pickles JR, Blundy JD, Brooker RA (2016) Trace element thermometry of garnet-clinopyroxene pairs. Am Mineral 101:1438–1450

Pokhilenko NP, Sobolev NV, Lavrent'ev YuG (1977) Xenoliths of diamondiferous ultramafic rocks from Yakutian kimberlites. 2nd Int Kimberlite Conf Ext Abs: pages not numbered

Pokhilenko NP, Sobolev NV, Reutsky VN, Hall AE, Taylor LA (2004) Crystalline inclusions and C isotope ratios in diamonds from the Snap Lake/King Lake kimberlite dyke system: evidence of ultradeep and enriched lithospheric mantle. Lithos 77:57–67

Ponomarenko AI, Spetsius ZV, Sobolev NV (1980) New type of diamond-bearing rock - pyroxenite. Dokl Akad Nauk SSSR 251:438–441

Purwin H, Lauterbach S, Brey GP, Woodland AB, Kleebe H-J (2013) An experimental study of the Fe oxidation states in garnet and clinopyroxene as a function of temperature in the system CaO–FeO–Fe_2O_3–MgO–Al_2O_3–SiO_2: implications for garnet–clinopyroxene geothermometry. Contrib Mineral Petrol 165:623–639

Rickard RS, Harris JW, Gurney JJ, Cardoso P (1989) Mineral inclusions from Koffiefontein mine. *In*: Kimberlites and Related Rocks. Ross J et al. (eds) Geol Soc Australia Spec Publ Spec Publ 14. Blackwell, Carlton, p 1054–1062
Ryan CG, Griffin WL, Pearson NJ (1996) Garnet geotherms: Pressure–temperature data from Cr-pyrope garnet xenocrysts in volcanic rocks. J Geophys Res 101:5611–5625
Schulze DJ, Coopersmith HG, Harte B, Pizzolato L-A (2008) Mineral inclusions in diamonds from the Kelsey Lake Mine, Colorado, USA: Depleted Archean mantle beneath the Proterozoic Yavapai province. Geochim Cosmochim Acta 72:1685–1695
Scott Smith BH, Danchin RV, Harris JW, Stracke KJ (1984) Kimberlites near Orroroo, South Australia. *In*: Kimberlites I: Kimberlites and Related Rocks. Kornprobst, J (ed) Elsevier, Amsterdam, p 121–142
Shatskii VS, Zedgenizov DA, Ragozin AL (2010) Majoritic garnets in diamonds from placers of the northeastern Siberian Platform. Doklady Earth Sci 432:835–838
Shatsky VS, Zedgenizov DA, Ragozin AL, Kalinina VV (2015) Diamondiferous subcontinental lithospheric mantle of the northeastern Siberian Craton: Evidence from mineral inclusions in alluvial diamonds. Gondwana Res 28:106–120
Shee SR, Gurney JJ, Robinson DN (1982) Two diamond-bearing peridotite xenoliths from the Finsch kimberlite, South Africa. Contrib Mineral Petrol 81:79–87
Shirey SB, Richardson SH (2011) Start of the Wilson cycle at 3 Ga shown by diamonds from subcontinental mantle. Science 333:434–436
Shirey SB, Cartigny P, Frost DJ, Keshav S, Nestola F, Nimis P, Pearson DG, Sobolev NV, Walter MJ (2013) Diamonds and the Geology of Mantle Carbon. *In*: Carbon in Earth. Hazen RM, Jones AP, Baross JA (eds) Rev Mineral Geochem 75:355–421
Simakov SK (2008) Garnet–clinopyroxene and clinopyroxene geothermobarometry of deep mantle and crust eclogites and peridotites. Lithos 106:125–136
Simakov SK, Taylor LA (2000) Geobarometry for mantle eclogites: solubility of Ca-Tschermaks in clinopyroxene. Int Geol Rev 42:534–544
Smith D, Griffin W, Ryan C, Sie S (1991) Trace-element zonation in garnets from The Thumb: heating and melt infiltration below the Colorado Plateau. Contrib Mineral Petrol 107:60-79
Smith CB, Pearson DG, Bulanova GP, Beard AD, Carlson RW, Wittig N, Sims K, Chimuka L, Muchemwa E (2009) Extremely depleted lithospheric mantle and diamonds beneath the southern Zimbabwe Craton. Lithos 112:1120–1132
Smith CB, Walter MJ, Bulanova GP, Mikhail S, Burnham AD, Gobbo L, Kohn SC (2016) Diamonds from Dachine, French Guiana: A unique record of early Proterozoic subduction. Lithos 265:82–95
Sobolev NV (1977) Deep-Seated Inclusions in Kimberlites and the Problem of the Composition of the Upper Mantle. Am Geophys Un, Washington, DC
Sobolev NV, Yefimova ES (1998) Compositional variations of chromite inclusions as an indicator of the zonation of diamond crystals. Dokl Earth Sci 359:163–166
Sobolev NV, Botkunov AI, Lavrent'ev YG, Usova LV (1976) New data on the minerals associated with the diamonds in the "Mir" kimberlite pipe in Yakutia. Geologiya I Geofizika, 17:1–10
Sobolev NV, Kaminsky FV, Griffin WL, Yefimova ES, Win TT, Ryan CG, Botkunov AI (1997a) Mineral inclusions in diamonds from the Sputnik kimberlite pipe, Yakutia. Lithos 39:135–157
Sobolev NV, Yefimova ES, Reimers LF, Zakharchenko OD, Makhin AI, Usova LV (1997b) Mineral inclusions in diamonds of the Arkhangelsk kimberlite province. Russ Geol Geophys 38:379–393
Sobolev NV, Yefimova ES, Koptil VL (1999) Mineral inclusions in diamonds in the Northeast of the Yakutian diamondiferous province. *In*: The P.H. Nixon Volume, Proc VIIth Int Kimberlite Conf. Gurney JJ, Gurney JL, Pascoe MD, Richardson SH (eds) Red Roof Design, Cape Town, p 816–822
Sobolev NV, Logvinova AM, Zedgenizov DA, Seryotkin YV, Yefimova ES, Floss C, Taylor LA (2004) Mineral inclusions in microdiamonds and macrodiamonds from kimberlites of Yakutia: a comparative study. Lithos 77:225–242
Sobolev NV, Logvinova AM, Zedgenizov DA, Pokhilenko NP, Kuzmin DV, Sobolev AV (2008) Olivine inclusions in diamonds: high-precision approach to minor elements. Eur J Mineral 20:305–315
Sobolev NV, Logvinova AM, Efimova ES (2009) Syngenetic phlogopite inclusions in kimberlite-hosted diamonds: implications for role of volatiles in diamond formation. Russ Geol Geophys 50:1234–1248
Stachel T (2014) Diamonds. Mineral Ass Can Short Course 44:1–28
Stachel T, Harris JW (1997a) Syngenetic inclusions in diamond from the Birim field (Ghana) - A deep peridotitic profile with a history of depletion and re-enrichment. Contrib Mineral Petrol 127:336–352
Stachel T, Harris JW (1997b) Diamond precipitation and mantle metasomatism – evidence from the trace element chemistry of silicate inclusions in diamonds from Akwatia, Ghana. Contrib Mineral Petrol 129:143–154
Stachel T, Harris JW (2008) The origin of cratonic diamonds - constraints from mineral inclusions. Ore Geol Rev 34:5–32
Stachel T, Luth RW (2015) Diamond formation—where, when and how? Lithos 220–223:200–220
Stachel T, Harris JW, Brey GP (1998) Rare and unusual mineral inclusions in diamonds from Mwadui, Tanzania. Contrib Mineral Petrol 132:34–47
Stachel T, Harris JW, Brey GB, Joswig W (2000) Kanakan diamonds (Guinea) II: lower mantle inclusion parageneses. Contrib Mineral Petrol 140:16–27
Stachel T, Harris JW, Tappert R, Brey GP (2003) Peridotitic diamonds from the Slave and the Kaapvaal cratons — similarities and differences based on a preliminary data set. Lithos 71:489–503

Stachel T, Viljoen KS, McDade P, Harris JW (2004) Diamondiferous lithospheric roots along the western margin of the Kalahari Craton—the peridotitic inclusion suite in diamonds from Orapa and Jwaneng. Contrib Mineral Petrol 147:32–47

Stachel T, Banas A, Muelenbachs K, Kurslaukis S, Walker EC (2006) Archean diamonds from Wawa (Canada): samples from deep cratonic roots predating cratonization of the Superior Province. Contrib Mineral Petrol 151:737–750

Stachel T, Banas A, Aulbach S, Smit KV, Wescott P, Chinn IL, Kong J (2018) The Victor Mine (Superior Craton, Canada): Neoproterozoic lherzolitic diamonds from a thermally modified cratonic root. Mineral Petrol 112 (Suppl 1) S325–S336

Sudholz ZJ, Yaxley GM, Jaques AL, Chen J (2021a) Ni-in-garnet geothermometry in mantle rocks: a high pressure experimental recalibration between 1100 and 1325 °C. Contrib Mineral Petrol 176:32

Sudholz ZJ, Yaxley GM, Jaques AL, Brey GP (2021b) Experimental recalibration of the Cr-in-clinopyroxene geobarometer: improved precision and reliability above 4.5 GPa. Contrib Mineral Petrol 176:11

Sun C, Liang Y (2015) A REE-in garnet-clinopyroxene thermobarometer for eclogites, granulites and garnet peridotites. Chem Geol 393–394:79–92

Tao R, Fei Y, Bullock ES, Xu C, Zhang L (2018) Experimental investigation of Fe^{3+}-rich majoritic garnet and its effect on majorite geobarometer. Geochim Cosmochim Acta 225:1–16

Tappert R, Stachel T, Harris JW, Muelenbachs K, Ludwig T, Brey GP (2005) Diamonds from Jagersfontein (South Africa): messengers from the sublithospheric mantle. Contrib Mineral Petrol 150:505–522

Tappert R, Stachel T, Harris JW, Muehlenbachs K, Brey GF (2006) Placer diamonds from Brazil: Indicators of the composition of the Earth's mantle and the distance to their kimberlitic sources. Econ Geol 101:453–470

Taylor WR (1998) An experimental test of some geothermometer and geobarometer formulations for upper mantle peridotites with application to the thermobarometry of fertile lherzolite and garnet websterite. N Jb Miner Abh 172:381–408

Taylor WR, Jacques AL, Ridd M (1990) Nitrogen-defect aggregation characteristics of some Australasian diamonds, Time-temperature constraints on the source regions of the pipe and alluvial diamonds. Am Mineral 75:1290–1310

Taylor WR, Canil D, Milledge HJ (1996) Kinetics of Ib to IAa nitrogen aggregation in diamond. Geochim Cosmochim Acta 60:4725–4733

Thomson AR, Kohn SC, Bulanova GP, Smith CB, Araujo D, EIMF, Walter MJ (2014) Origin of sub-lithospheric diamonds from the Juina-5 kimberlite (Brazil): constraints from carbon isotopes and inclusion compositions. Contrib Mineral Petrol 168:1081

Thomson AR, Walter MJ, Kohn SC, Brooker RA (2016) Slab melting as a barrier to deep carbon subduction. Nature 529:76–79

Thomson AR, Kohn SC, Prabhu A, Walter MJ (2021) Evaluating the formation pressure of diamond-hosted majoritic garnets: A machine learning majorite barometer. J Geophys Res: Solid Earth 126:e2020JB020604

Tsai H, Meyer HOA, Moreau J, Milledge HJ (1979) Mineral inclusions in diamond: Premier, Jagersfontein and Finsch kimberlites, South Africa, and Williamson Mine, Tanzania. *In*: Kimberlites, Diatremes, and Diamonds: their Geology, Petrology, and Geochemistry. Proc 2nd Int Kimberlite Conf. Boyd FR, Meyer HOA (eds) Am Geophys Un, Washington, DC, p 16–26

Van Rythoven AD, Schulze DJ (2009) In-situ analysis of diamonds and their inclusions from the Diavik mine, Northwest Territories, Canada: mapping diamond growth. Lithos 112:870–879

Van Rythoven AD, McCandless TE, Schulze DJ, Bellis A, Taylor LA, Liu Y (2011) Diamond crystals and their mineral inclusions from the Lynx kimberlite dyke complex, central Quebec. Can Mineral 49:691–706

Viljoen KS, Swash PM, Otter ML, Schulze DJ, Lawless PJ (1992) Diamondiferous garnet harzburgites from the Finsch kimberlite, Northern Cape, South Africa. Contrib Mineral Petrol 110:133–138

Viljoen KS, Harris JW, Ivanic T, Richardson SH, Gray K (2014) Trace element chemistry of peridotitic garnets in diamonds from the Premier (Cullinan) and Finsch kimberlites, South Africa: contrasting styles of mantle metasomatism. Lithos 208:1–15

Viljoen KS, Perritt SH, Chinn IL (2018) An unusual suite of eclogitic, websteritic and transitional websteritic-lherzolitic diamonds from the Voorspoed kimberlite in South Africa: mineral inclusions and infrared characteristics. Lithos 320–321:416–434

Walter MJ, Kohn SC, Araujo D, Bulanova GP, Smith CB, Gaillou E, Wang J, Steele A, Shirey SB (2011) Deep mantle cycling of oceanic crust: evidence from diamonds and their mineral inclusions. Science 334:54–57

Walter MJ, Thomson AR, Smith EM (2022) Geochemistry of silicate and oxide inclusions in sublithospheric diamonds. Rev Mineral Geochem 88:393–450

Wang WY, Sueno S, Takahashi E, Yurimoto H, Gasparik T (2000) Enrichment processes at the base of the Archean lithospheric mantle: observations from trace element characteristics of pyropic garnet inclusions in diamonds. Contrib Mineral Petrol 139:720–733

Webb SAC, Wood BJ (1986) Spinel-pyroxene-garnet relationships and their dependence on Cr/Al ratio. Contrib Mineral Petrol 92:471–480

Weiss Y, Navon O, Goldstein SL, Harris JW (2018) Inclusions in diamonds constrain thermo-chemical conditions during Mesozoic metasomatism of the Kaapvaal cratonic mantle. Earth Planet Sci Lett 491:134–147

Wijbrans CH, Rohrbach A, Klemme S (2016) An experimental investigation of the stability of majoritic garnet in the Earth's mantle and an improved majorite geobarometer. Contrib Mineral Petrol 171:50

Wilding MC (1990) A study of diamonds with syngenetic inclusions. PhD thesis, University of Edinburgh, Scotland, UK
Wilding MC, Harte B, Fallick AE, Harris JW (1994) Inclusion chemistry, carbon isotopes and nitrogen distribution in diamonds from the Bultfontein Mine, South Africa. *In*: Diamonds: Characterization, Genesis and Exploration. Meyer HOA, Leonardos OH (eds) CPRM Spec Publ Jan/94, Brasilia, p 116–126
Witt-Eickschen G, O'Neill H (2005) The effect of temperature on the equilibrium distribution of trace elements between clinopyroxene, orthopyroxene, olivine and spinel in upper mantle peridotite. Chem Geol 221:65–101
Woodland AB (2009) Ferric iron contents of clinopyroxene from cratonic mantle and partitioning behaviour with garnet. Lithos 112S:1143–1149
Woodland AB, Girnis AV, Bulatov VK, Brey GP, Höfer HE (2020) Breyite inclusions in diamond: experimental evidence for possible dual origin. Eur J Mineral 32:171–185
Wu CM, Zhao GC (2007) A recalibration of the garnet–olivine geothermometer and a new geobarometer for garnet peridotites and garnet–olivine–plagioclase-bearing granulites. J Metamorph Geol 25:497–505
Zedgenizov DA, Kagi H, Shatsky VS, Ragozin AL (2014) Local variations of carbon isotope composition in diamonds from São-Luis (Brazil): Evidence for heterogenous carbon reservoir in sublithospheric mantle. Chem Geol 363:114–124
Zhang Z, Ganguly J, Ito M (2010) Ca–Mg diffusion in diopside: tracer and chemical inter-diffusion coefficients. Contrib Mineral Petrol 159:175–186
Ziberna L, Klemme S, Nimis P (2013) Garnet and spinel in fertile and depleted mantle: insights from thermodynamic modelling. Contrib Mineral Petrol 166:411–421
Ziberna L, Nimis P, Kuzmin D, Malkovets VG (2016) Error sources in single-clinopyroxene thermobarometry and a mantle geotherm for the Novinka kimberlite, Yakutia. Am Mineral 101:2222–2232